T.R.

GEBZE TECHNICAL UNIVERSITY

GRADUATE SCHOOL OF NATURAL AND APPLIED SCIENCES

NUMERICAL ANALYSIS OF SPECTRAL COLLOCATION METHOD FOR MAGNETOHYDRODYNAMIC EQUATIONS

ALI RIDWANOU SERAJOU

A THESIS SUBMITTED FOR THE DEGREE OF

MASTER OF SCIENCE

DEPARTMENT OF MATHEMATICS

GEBZE

2019

T.R.

GEBZE TECHNICAL UNIVERSITY

GRADUATE SCHOOL OF NATURAL AND APPLIED SCIENCES

NUMERICAL ANALYSIS OF SPECTRAL COLLOCATION METHOD FOR MAGNETOHYDRODYNAMIC EQUATIONS

ALI RIDWANOU SERAJOU

A THESIS SUBMITTED FOR THE DEGREE OF

MASTER OF SCIENCE

DEPARTMENT OF MATHEMATICS

THESIS SUPERVISOR

ASSIST. PROF. DR. ÖNDER TÜRK

GEBZE

2019

T.C.
GEBZE TEKNİK ÜNİVERSİTESİ
FEN BİLİMLERİ ENSTİTÜSÜ

SPEKTRAL KOLOKASYON METODUNUN MANYETOHİDRODİNAMİK DENKLEMLER İÇİN SAYISAL ANALİZİ

ALİ RİDWANOU SERAJOU
YÜKSEK LİSANS TEZİ MATEMATİK
ANABİLİM DALI

DANIŞMANI
DR. ÖĞR. ÜYESİ ÖNDER TÜRK

GEBZE
2019

GEBZE TEKNİK ÜNİVERSİTESİ	**YÜKSEK LİSANS JÜRİ ONAY FORMU**

GTÜ Fen Bilimler Enstitüsü Yönetim Kurulu'nun ..03../04.../2019 tarih ve ..2019./.17...... sayılı kararıyla oluşturulan jüri tarafından ...10../..04../2019. tarihinde tez savunma sınavı yapılan Ali Ridwanou SERAJOU'ın tez çalışması Matematik Anabilim Dalında YÜKSEK LİSANS tezi olarak kabul edilmiştir.

JÜRİ

ÜYE
(TEZ DANIŞMANI) : Dr. Öğr. Üyesi Önder TÜRK

ÜYE : Prof. Dr. Mansur İSGENDEROĞLU

ÜYE : Dr. Öğr. Üyesi Cengiz ERDÖNMEZ

ONAY

Gebze Teknik Üniversitesi Fen Bilimleri Enstitüsü Yönetim Kurulu'nun

....../....../......... tarih ve ..../........ sayılı kararı.

SUMMARY

In this thesis, the numerical solutions of magnetohydrodynamic (MHD) flow problems using Chebyshev spectral collocation method (CSCM) are presented. The CSCM mainly depends on polynomial interpolation, and the differentiation of the polynomial that approximates the function which is under consideration. Therefore, the polynomial interpolation theory with salient results is investigated. The interpolation properties of polynomials by means of Lebesgue constant which provides a way to analyze the Lagrange interpolation polynomial by determining its closeness to the best approximating polynomial are also investigated. For this, three sets of points namely, the equispaced points, the Chebyshev Gauss (CG) points, and the Chebyshev Gauss Lobatto (CGL) points are considered, and the associated Lebesgue constants are evaluated to determine interpolation aspects of the choice of interpolation points. Thereafter, approximating the derivative of a function which is a solution to a given differential equation is taken into consideration.

The accuracy of CSCM methodology is analyzed by solving one-dimensional and two-dimensional laminar flow problems of incompressible viscous fluids. A simple one-dimensional flow problem known as MHD Couette flow that relies on the interaction of electric, magnetic, and hydrodynamic forces in the fluid, is studied to explore the convergence properties of the method. Moreover, two-dimensional MHD flow problems, subjected to an externally applied magnetic field, with a novel solution strategy designed to take account the induced magnetic field in a non-singular lid-driven cavity is introduced. The obtained numerical results indicate that the designed procedure effectively approximates the full MHD equations by following a discretization in the physical space, and of moderate size. Moreover, the divergence-free nature of the magnetic field is shown to be preserved on the whole computational domain.

Keywords: Chebyshev interpolation, CSCM, MHD flow, Divergence-free field.

ÖZET

Bu tez çalışmasında Chebyshev spektral kolokasyon yöntemi (CSCM) kullanılarak manyetohidrodinamik (MHD) akış problemlerinin sayısal çözümleri sunulmuştur. Bu metot esas olarak ele alınan bir fonksiyon ve bu fonksiyonun türevinin interpolasyon polinomuyla yaklaşık olarak hesaplanmasına bağlıdır. Bu gerekçeyle, çalışmada polinom interpolasyon teorisi ve bu teorinin öne çıkan özellikleri incelenmiştir. Lagrange interpolasyon polinomunun belirli bir norma göre en iyi yaklaşık polinomu ile olan yakınlığını belirleyerek analiz etmek için bir yol sağlayan Lebesgue sabiti ile polinomların interpolasyon özellikleri de incelenmiştir. Bunun için, eşit aralıklı noktalar, Chebyshev Gauss (CG) noktaları ve Chebyshev Gauss Lobatto (CGL) noktaları olmak üzere üç ayrıklaştırma göz önünde bulundurulmuş ve ilgili Lebesgue sabitleri karşılaştırılmıştır. Daha sonra, belirli bir diferansiyel denklemin çözümü olan bir fonksiyonun türevinin yaklaşık olarak hesaplanması ele alınmıştır.

CSCM metodolojisinin doğruluğu, sıkıştırılamaz viskoz akışkanların bir boyutlu ve iki boyutlu laminer akış problemlerini çözerek analiz edilmiştir. Akışkandaki elektrik, manyetik ve hidrodinamik kuvvetlerin etkileşimine dayanan MHD Couette akışı olarak bilinen bir boyutlu akış problemi, yöntemin yakınsaklık özelliklerini incelemek üzere ele alınmıştır. Ayrıca, harici olarak uygulanan bir manyetik alan etkisi altında iki boyutlu MHD akış problemleri, tekil olmayan bir duvarı hareketli kanal problemi üzerinde indüklenen manyetik alanı modele dahil edebilmek için tasarlanan yeni bir çözüm stratejisi ortaya konmuştur. Elde edilen sayısal sonuçlar, tasarlanan prosedürün, fiziksel alanda ve orta büyüklükte bir ayrıklaştırma izleyerek tam MHD denklemlerine etkili bir şekilde yaklaşık sonuçlar elde edildiğini göstermiştir. Ayrıca, manyetik alanın serbest-diverjans özelliğinin bütün problem bölgesi üzerinde korunduğu gösterilmiştir.

Anahtar Kelimler: Chebysev interpolasyonu, CSCM, MHD akışı, Serbest-diverjans alan.

ACKNOWLEDGEMENTS

First of all, I thank God for guiding me through my education and giving me good health, patience and perseverance that were necessary to complete this thesis. I would like to acknowledge my warmest thanks to my supervisor Assist. Prof. Dr. Önder TÜRK, who not only shared his profound scientific knowledge with me but also taught me great lessons of life. His friendly guidance and expert advice have been invaluable throughout all stages of the work. His door was always open whenever I had a question about my research or writing. It has been a privilege and great experience to work with him. I would also like to thank Prof. Dr. Mansur İSGENDEROĞLU for his advice and encouragement during this work. My sincere thanks also goes to Assist. Prof. Dr. Cengiz ERDÖNMEZ for being part of my thesis committee. Moreover, I would like to thank Prof. Dr. Coşkun YAKAR for his advice. I thank YTB Scholarships for giving me the opportunity to study in Turkey.

Special thanks are due to my parents, Mouhamadou SERAJOU and Awa OUSMAROU who have provided me through love, moral, encouragement, and emotional support in my life. They are the ultimate role models. I am also grateful to my other family members and friends for supporting me spiritually throughout writing this thesis.

Last but not the least, I want to thank my loving and wonderful daughter Majda ALI RIDWANOU for her patience during my absence.

TABLE of CONTENTS

LIST of ABBREVIATIONS and ACRONYMS

Abbreviations and Acronyms		**Explanations**
Δ	:	Laplace operator
ψ	:	Stream function
w	:	Vorticity
$\boldsymbol{A}$	:	Magnetic stream function
$\boldsymbol{J}$	:	Current density
$\mathbf{B}$	:	Magnetic field
$\mathbf{E}$	:	Electric field
$\mathbf{V}$	:	Velocity field
Λ_N	:	Lebesgue constant
$\lambda_N(x)$	:	Lebesgue function
p	:	Pressure
ρ	:	Density
ρ_c	:	Free electric charge density
ξ	:	Electric permittivity
μ_m	:	Magnetic permeability
υ	:	Kinematic viscosity
χ_b	:	The body force
χ_{ext}	:	Extern force due to the body force and the Lorentz force
σ	:	Electric conductivity
$\mathfrak{D}$	:	Differential operator
$\mathfrak{B}$	:	Boundary operator
$\otimes$	:	Kronecker product
$[D_N^{(m)}]$	:	The m-th order Chebyshev spectral differentiation matrix
D	:	Diagonal matrix
ι	:	The vector of order $(N+1)^2$ whose all entries are 1
C[a,b]	:	The set of continuous functions on [a,b]
Ha	:	Hartmann number
Re	:	Reynolds number
Re_m	:	Magnetic Reynolds number

Al	:	Alfvren number
$C_k(x)$	:	Cardinal function (or Lagrange basis)
$T_N(x)$	:	Chebyshev polynomial of degree N
$w(x)$	:	Weight function
x_j CGL	:	Chebyshev Gauss Lobatto points
2D	:	Two-Dimensional
MHD	:	Magnetohydrodynamic
CSCM	:	Chebyshev Spectral Collocation Method
CG	:	Chebyshev Gauss
CGL	:	Chebyshev Gauss Lobatto
CFD	:	Computational Fluid Dynamics
N-S	:	Navier – Stokes
PDEs	:	Partial Differential Equations
FDM	:	Finite Difference Method
FEM	:	Finite Element Method
FVM	:	Finite Volume Method
CDM	:	Chebyshev Differentiation Matrix

LIST of FIGURES

LIST of TABLES

1. INTRODUCTION

1.1. Subject And Purpose Of The Thesis

Many problems within industrial, engineering and scientific areas that are defined by partial differential equations (PDEs) do not have analytical solutions. Analytical methods are mostly applied in some simplified flow problems in simple geometries. There is therefore the significant need for developing efficient and accurate numerical techniques for solving these PDEs. Computational fluid dynamics (CFD) is a research area which involves the applications of numerical analysis in fluid dynamics, and often requires the use of discretized PDEs. CFD, fundamentally purposes to solve numerically complex problems of fluid dynamics which emanate from disciplines such as chemical process engineering, ocean engineering, aerodynamics, and air pollution modeling. There is a large number of computational tools used in CFD. However, there are ongoing studies to improve the numerical methods and the physical methods. Many solution methodologies exist in solving flow problems which include finite difference method (FDM), finite volume method (FVM), and spectral methods. With the advantage of numerical computation machines, notably computers, these methods have now become an essential tools for solving many fundamental problems of scientific phenomena which were difficult to solve in the past.

Spectral methods are generally defined as a family of numerical methods in which a function is globally approximated by representing it as a finite sum of orthogonal functions preassigned. In these methods, each function spans the entire domain under consideration. Consequently, the derivatives of the function depend on the whole discretization. The most characteristic property of these methods is the global approximation feature. Furthermore, the derivatives of polynomials previously assigned approximate the spatial derivatives of the solution. A subclass of the spectral methods is the spectral collocation method also known as pseudo-spectral method and is similar to FDM in the direct use of a set of grid points namely, collocation points.

The Chebyshev spectral collocation method (CSCM) is an example where the interpolating polynomials are defined on a set of points in which the differential equations are discretized to approximate the unknown functions. The polynomials are analytically differentiated, and for derivative approximation a differentiation matrix is constructed. The collocation points in this method are taken as the Chebyshev Gauss Lobatto (CGL) points that are the extreme points of the Chebyshev polynomials in $[-1,1]$.

Essentially, the CSCM depends on polynomial interpolation and the differentiation of this polynomial that approximates the function under consideration. Therefore, in this study the interpolation theory to some extent will be detailed in Chapter 2. As a matter of fact, these results are known, and fully available in the literature, however, we collect them in Chapter 2 to enlighten the theory behind the CSCM. To do this, the Lagrange interpolation polynomial with equispaced points is introduced after which the existence and uniqueness of interpolation polynomial is proved. Next, Weierstrass theorem which asserts that any continuous real valued function on $[a,b]$ can be approximated to any accuracy by polynomials is also introduced and proved. Thereafter, the Runge phenomenon which is a complication that emerges when approaching a function with polynomials of high degree over a set of equally spaced interpolation points is discussed. Then, the solution to the problem arising from this phenomenon is considered by choosing special points. Next, Chebyshev polynomials as well as the points to be used in the interpolation are also presented. Polynomial approximation in the infinity norm is used to determine differences in the function and its interpolating polynomial. Consequently, the best approximation of a fixed degree is stated with examples. Moreover, the Lebesgue function which is the summation of the absolute value of Lagrange basis functions, as well as its maximum over the domain of interpolation called the Lebesgue constant are evaluated. The Lebesgue constant, defined as the maximum of Lebesgue function depends on the interpolation points, and gives an idea to how far in a working norm, the Lagrange interpolation polynomial is from the best approximation polynomial. For this purpose, three sets of points, namely, the equispaced points, the Chebyshev Gauss (CG) points, and the CGL points are investigated in terms of Lebesgue constant to determine their interpolation properties. With regard to the application of CSCM, differentiation of interpolation polynomial is presented and illustrated by examples.

There are several advantages of spectral methods over alternative approaches, such as finite element method (FEM) or FDM. The characteristic specialty of the spectral methods is the high precision resulting from the high order approximation compared to local methods where the solution at a particular node is affected by a limited number of points around it. Their main advantage is the convergence rate that depends on the smoothness of the solution, and the number of continuous derivatives admitted by the solution. The error in the spectral method solution decreases exponentially for infinitely smooth solution. Over the last decades, the implementation of spectral methods for applications such as CFD has broaden.

Magnetohydrodynamic (MHD) flows are of great importance for many researches. MHD which is the coupling between electro-magnetism and hydrodynamics, combines elements of electro-magnetism and fluid mechanics to define the flow of electrically conducting fluids. The MHD equations are obtained by coupling the Navier-Stokes (N-S) equations with Maxwell's equations by using Ohm's law. In literature, there are studies solving MHD equations with several numerical methods. In general, these methods produce results which do not satisfy the divergence-free condition. Therefore, the ultimate objective of this study is to solve MHD equations numerically using CSCM with a methodology that produces results in such a way the physical properties are satisfied.

1.2. Formulation Of MHD Flow Equations

In this section, the MHD flow of an incompressible, steady, and electrically conducting fluid is considered. As mentioned before, the MHD equations are governed by Maxwell's equations and N-S equations. Maxwell's equations which are the combination of laws of electromagnetism are given as follows [1]-[2]

$$\nabla \times \mathbf{E} = 0 \qquad \text{(Faraday's law)} \tag{1.1}$$

$$\nabla \times \mathbf{H} = J \qquad \text{(Ampere's law)} \tag{1.2}$$

$$\nabla . \mathbf{D} = \rho_c \qquad \text{(Gauss's law)} \tag{1.3}$$

$$\nabla . \mathbf{B} = 0 \qquad \text{(Gauss magnetism's law)} \tag{1.4}$$

where $\mathbf{E}$ is the electric field, $\mathbf{J}$ and $\mathbf{H}$ are the current density and the magnetic field strength, respectively. $\mathbf{D}$ is the time rate of electric displacement field, ρ_c is the free electric charge density, and $\mathbf{B}$ is the magnetic induction. For the free space, the relations

$$\mathbf{D} = \xi \mathbf{E} \quad \text{and} \quad \mathbf{B} = \mu_m \mathbf{H} \tag{1.5}$$

are valid, where ξ is the electric permittivity, and μ_m is the magnetic permeability. The N-S equations are given as

$$\nabla.\mathbf{V} = 0 \qquad \text{(Continuity equation)} \tag{1.6}$$

$$\mathbf{V}\nabla.\mathbf{V} = -\frac{1}{\rho}\nabla p + \upsilon \Delta \mathbf{V} + \chi_{ext} \quad \text{(Momentum equation)} \tag{1.7}$$

where Δ is the Laplace operator, $\mathbf{V}$ is the velocity field, ρ is the density, p is the pressure, υ is the kinematic viscosity, and χ_{ext} is the force applied externally which is a totalization of body forces and the Lorentz force $(\nabla \times \mathbf{B}) \times \mathbf{B}$. These equations are associated with Maxwell's equations given above using Ohm's law

$$\mathbf{J} = \sigma(\mathbf{E} + \mathbf{V} \times \mathbf{B}), \tag{1.8}$$

where σ is the electrical conductivity. Combining Equations (1.1)-(1.8), a steady, incompressible MHD flow governing equations are written in non-dimensional form as [3]

$$\begin{aligned}
\nabla.\mathbf{u} &= 0, \\
\nabla.\mathbf{b} &= 0, \\
-\nabla \times (\mathbf{u} \times \mathbf{b}) &= \frac{1}{Re_m}\Delta \mathbf{b}, \\
\mathbf{u}.\nabla \mathbf{u} &= -\nabla p + \frac{1}{Re}\Delta \mathbf{u} + Al(\nabla \times \mathbf{b}) \times \mathbf{b} + \chi_b,
\end{aligned} \tag{1.9}$$

where χ_b is the body force, $\mathbf{u}$ the velocity field, p the pressure, and $\mathbf{b}$ the magnetic field. Re_m is the magnetic Reynolds number defined as $Re_m = \sigma \mu_m LU$, where L is the characteristic length and, U the characteristic velocity. Al is the Alfvren number which is defined as $Al = \mathbf{B}^2/p\mu_m U^2$, where $\mathbf{B}$ is the characteristic magnetic induction. Re is the Reynolds number defined as $Re = LU/\upsilon$.

A solution methodology to approximate the solution to these equations in several physical configurations will be presented in Chapter 3.

1.3. Literature Survey

MHD is a branch of science which combines electromagnetism elements and fluid mechanics to define the flow of electrically conducting fluids. Because of the wide range of significant applications in various fields such as MHD generators, nuclear reactors, and metallurgical industries, MHD flow of electrically conducting fluids in the presence of magnetic field in enclosures has been the subject of a great number of theoretical, experimental, and numerical investigations. The physical models that describe MHD flow consist of coupling the problem of magnetic field in N-S equations with Lorentz's force, and Maxwell's equations of electromagnetics using Ohm's law. Extensive research is ongoing in the direction of designing numerical techniques applicable to the MHD flow and viscous incompressible laminar flow as the analytical solutions apply only under some special conditions. In majority of the studies, the aim is to determine the influence of the characteristic problem parameters such as Reynolds, magnetic Reynolds, and Hartmann numbers on the flow. In general, the governing equations can only be solved numerically because of their nonlinearity and the additional terms due to the existence of Lorentz's force. Another restriction comes from the divergence-free constraint for both the magnetic and the velocity fields. Therefore, to develop accurate and effective numerical methods is a challenging task. Many different numerical methods have been introduced for approximating solutions to MHD flow and viscous incompressible laminar flow.

In [4], the primitive variable formulation of full MHD equations have been approximated by using a second order FDM combining the MAC scheme for the N-S equation with the Yee's scheme for the Maxwell equations without taking into account the divergence-free condition (1.4) in the numerical model. An approximate solution of the incompressible MHD flow equations have been given in [1] using a dual reciprocity boundary element method. A stabilized FEM solution to the MHD problem with thermal coupling has been proposed in [5]. A numerical solution using FEM for the approximation of laminar, steady, natural convection flow in inclined enclosures under the influence of an oblique magnetic field has been given in [6]. In [7], a dual reciprocity boundary element solution for full MHD equations has been proposed in a lid driven square cavity. In [8] a numerical solution using a fourth order finite difference algorithm has been proposed for the solution of incompressible steady full MHD equations formulated in stream function, velocity, and magnetic induction. In a recent study [9], a solution for the full MHD equations coupled with energy equations has been proposed using CSCM to approximate an unsteady, incompressible, laminar MHD problem with heat transfer using the Boussinesq approximation for thermal coupling.

2. THEORY OF INTERPOLATION

In this chapter, the polynomial interpolation, and the importance of the choice of interpolation points is presented. Determining the right choice of interpolation points is important because it allows for the precise approximation of functions. Numerical interpolation generally consists of approximating a function whose values are only known at certain points. More precisely, given $x_0, x_1, \ldots, x_N$, distinct real numbers, and $y_0, y_1, \ldots, y_N$ real numbers, the problem consists of finding an interpolation function Φ such that $\Phi(x_j) = y_j$ for $j = 0, \ldots, N$. Then, it is said that Φ interpolates y_j to points x_j. The form of the interpolation function Φ depends on the problem and the purpose of the interpolation. In fact, Φ can be a polynomial, in which case it is referred as polynomial interpolation, or Φ can be a piecewise polynomial function, and can also be said to be a piecewise interpolation. In this thesis, the case where Φ is a polynomial is considered. The reason for choosing Φ as a polynomial is that, polynomials can be calculated by elementary operations, may be differentiated and integrated without difficulty, and are simple in form. The interest and the mode of use of an interpolation function depends mainly on the origin of the data. The quantities y_j may, for example, represent the values at the points x_j of an analytically known function f. The interpolation function then makes it possible to simplify the numerical calculations of integrals or derivatives.

To begin with the interpolation idea, the Lagrange polynomial interpolation with equispaced points is introduced. Then the Runge phenomenon is discussed with the solution to the problem arising from this phenomenon is considered by choosing special points. To illustrate interpolation, exponential function and Runge's example are used and for Runge case, two different interpolation points are used with the help of Lagrange polynomials. The motivation to include these two cases is to illustrate how the choice of the interpolation points is important.

In the first section, the basic problem of polynomial interpolation is introduced, and the existence and uniqueness of the interpolation polynomial is proven. In certain cases, the interpolating polynomial can differ significantly from the function to be interpolated. This is illustrated first by Carl Runge, and it is called the Runge Phenomenon. The example due to Runge is presented along with a few results on convergence of the interpolating polynomials. Furthermore, Chebyshev polynomials as well as the points to be used in the interpolation will be also presented.

In the second section, the best approximation in the infinity norm with some theorems and examples are introduced. Next, Lebesgue function and Lebesgue constant are evaluated. Finally, differentiation is also presented and examples are given.

2.1. Polynomial Interpolation

In this section, the polynomial interpolation with some important properties and results are presented. For a non-negative integer N, let $\mathscr{P}_N$ be the set of all (real valued) polynomials of degree at most N defined over $\mathbb{R}$, it is obvious how to extend the theory for complex numbers. The goal in this section is to numerically approximate some smooth functions, and investigate their convergence properties. Thereafter, ways of choosing the interpolation points which results in an acceptable approximation.

Lemma 2.1. (*Existence of interpolating polynomial*)

Let $N \geq 1$. There exist polynomials $C_k \in \mathscr{P}_N$, $k = 0, 1, \ldots, N$, such that:

$$C_k(x_j) = \begin{cases} 1 & \text{if} \quad j = k \\ 0 & \text{otherwise} \end{cases} \qquad \forall j,k = 0,1,\ldots,N. \tag{2.1}$$

Furthermore,

$$p_N(x) = \sum_{k=0}^{N} C_k(x) y_k; \quad p_N \in \mathscr{P}_N, \tag{2.2}$$

is a polynomial such that $p_N(x_j) = y_j$.

Proof. *For k in the interval $[0, N]$, $C_k(x)$ has the form*

$$C_k(x) = \alpha_k \prod_{\substack{j=0 \\ j \neq k}}^{N} (x - x_j), \tag{2.3}$$

where $\alpha_k \in \mathbb{R}$ is a constant to be determined. From (2.3), to have $C_k(x_k) = 1$, it is set as $C_k(x_k) = \alpha_k \prod_{\substack{j=0 \\ j \neq k}}^{N} (x_k - x_j)$.

Therefore, it is obtained as $\alpha_k = \prod_{\substack{j=0\\ j\neq k}}^{N} \frac{1}{x_k - x_j}$. *Then,*

$$C_k(x) = \prod_{\substack{j=0\\ j\neq k}}^{N} \frac{x - x_j}{x_k - x_j}, \quad \text{for} \quad k = 0, 1, \ldots, N, \quad (C_k(x) \in \mathscr{P}_N). \tag{2.4}$$

Writing $p_N(x)$ *with* $p_N \in \mathscr{P}_N$, *and such that* $p_N(x) = \sum_{k=0}^{N} y_k C_k(x)$. *Thus,*

$$p_N(x_j) = y_0 \underbrace{C_0(x_j)}_{=0} + y_1 \underbrace{C_1(x_j)}_{=0} + \cdots + y_j \underbrace{C_j(x_j)}_{=1} + \cdots + y_N \underbrace{C_N(x_j)}_{=0}. \tag{2.5}$$

Hence, from (2.5) it is obtained that $p_N(x_j) = y_j$.

$\square$

As an example regarding the Lagrange basis functions, the following graphs in Figure 2.1 are illustrated. This figure presents the graphs of the Lagrange basis functions based on the equispaced (left) and CGL (right) points respectively for $N = 12$. It is observed that the graphs of Lagrange basis functions using equispaced points oscillates near the endpoints which is not the case of CGL points.

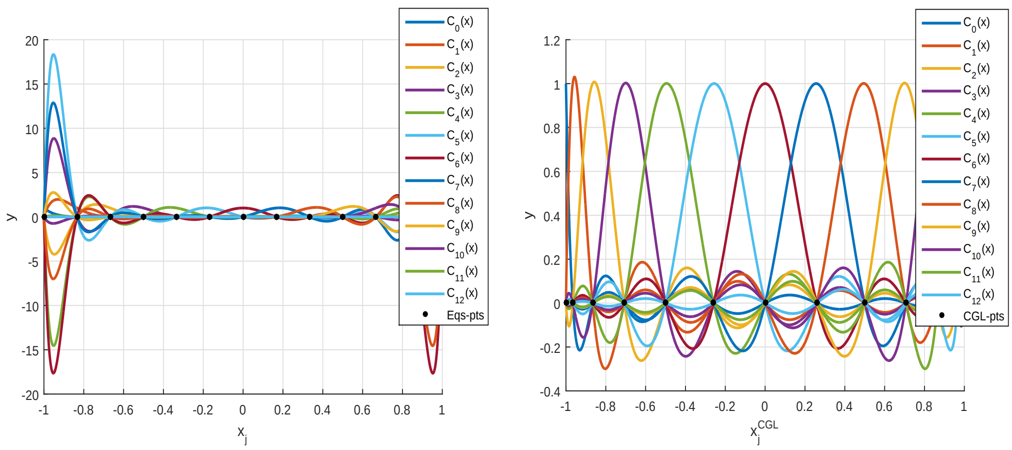

Figure 2.1: Graphs of Lagrange basis functions using equispaced (left) and CGL (right) points on $[-1, 1]$ for $N = 12$.

The interpolation polynomial is unique as asserted by the following theorem taken from [10].

Theorem 2.1. (*Uniqueness of interpolating polynomial*)

Suppose that $N \geq 0$. Let $x_0, x_1, \dots, x_N$, be distinct real numbers and $y_0, y_1, \dots, y_N$ be real numbers, then there is a unique polynomial $p_N \in \mathscr{P}_N$ so that $p_N(x_j) = y_j$, $j = 0, 1, \dots, N$.

Proof. *Suppose that $q_N(x) \in \mathscr{P}_N$ exists such that $q_N(x_j) = y_j,\ j = 0, 1, \dots, N$, different from $p_N(x) \in \mathscr{P}_N$. Let $\rho_N(x) = p_N(x) - q_N(x)$, this implies that $\rho_N(x) \in \mathscr{P}_N$ and, has $N+1$ distinct roots $x_0, x_1, \dots, x_N$. Since ρ_N is a polynomial of degree N, it can not have more than N distinct roots. Therefore, $\rho_N(x)$ is the zero polynomial, which contradicts the fact that q_N and p_N are distinct. Thus $p_N = q_N$. Hence, the interpolating polynomial is unique.*

□

Definition 2.1. (*Lagrange interpolation polynomial*)

Suppose that $N \geq 0$, given the real valued function $f \in C[a,b]$, where $C[a,b]$ is the set of continuous functions on $[a,b]$, and $x_j,\ j = 0, 1, \dots, N$, the distinct interpolation points, the polynomial p_N defined by

$$p_N(x) = \sum_{k=0}^{N} C_k(x) f(x_k), \tag{2.6}$$

is the Lagrange interpolation polynomial of degree N with interpolation points $x_j,\ j = 0, 1, \dots, N$, for the function f where $C_k(x)$ is the cardinal function (or Lagrange basis) defined in (2.4).

In providing estimates of the error that emerges in interpolating the function f, Theorem 2.2 is included below. The interpolant and the function are not expected to be close to each other at any point provided they both agree with each other at the points of interpolation. The difference between them on the interpolation domain which is referred to as the interpolation error given in [10] can however be estimated.

Theorem 2.2. (*Interpolation error*)

Suppose that $N \geq 0$, and $f \in C^{N+1}[a,b]$, then given $x \in [a,b]$, there exists $\zeta = \zeta(x)$ in (a,b) such that

$$f(x) - p_N(x) = \frac{f^{(N+1)}(\zeta)}{(N+1)!}\omega_{N+1}(x); \quad \omega_{N+1}(x) = (x - x_0)\cdots(x - x_N). \tag{2.7}$$

Moreover,

$$|f(x)-p_N(x)| \leq \frac{\Gamma_{N+1}}{(N+1)!}|\omega_{N+1}(x)|, \text{ where } \Gamma_{N+1} = \max_{a\leq\zeta\leq b}|f^{(N+1)}(\zeta)|. \tag{2.8}$$

The following examples are included to illustrate how Theorem 2.2 can be used to estimate the interpolation error.

Example 2.1. The function $f: x \mapsto e^x$ defined on $[-1,1]$ is considered. From this the Lagrange interpolation polynomial of degree 2 is constructed, and then Theorem 2.2 is verified.

In this case $N=2$, the interpolation points are $x_0=-1,\ \ x_1=0,\ \ $ and $x_2=1$. Then, $C_0(x), C_1(x)$, and $C_2(x)$ need to be determined. For $C_0(x)$ the following applies:

$$\begin{aligned} C_0(x) &= \frac{(x-x_1)(x-x_2)}{(x_0-x_1)(x_0-x_2)} \\ &= \frac{1}{2}x(x-1). \end{aligned} \tag{2.9}$$

For $C_1(x)$ the following applies:

$$\begin{aligned} C_1(x) &= \frac{(x+1)(x-1)}{1(-1)} \\ &= 1-x^2. \end{aligned} \tag{2.10}$$

For $C_2(x)$ the following applies:

$$\begin{aligned} C_2(x) &= \frac{(x+1)x}{2(1)} \\ &= \frac{1}{2}x(x+1). \end{aligned} \tag{2.11}$$

$f(x_0)=e^{-1},\quad f(x_1)=1$, and $f(x_2)=e$. By using the relation (2.6), and (2.9)-(2.11), it is obtained as: $p_2(x)=\frac{1}{2}x(x-1)e^{-1}+(1-x^2)+\frac{1}{2}x(x+1)e$.

Therefore, by using Theorem 2.2 it is obtained as:

$$\max_{-1\leq x\leq 1}|f(x)-p_2(x)| \leq \frac{\Gamma_3}{3!}|\omega_3(x)|, \quad \text{where } \Gamma_3 = \max_{-1\leq\zeta\leq 1}|f^{(3)}(\zeta)|. \tag{2.12}$$

From (2.12), the following applies $\max_{-1\leq x\leq 1}|f(x)-p_2(x)| \leq \frac{e}{3!}|x(x^2-1)| \leq \frac{e}{3!}=0.435$.

Hence, the estimation of the interpolation error with respect to the infinity norm on *the interval* $[-1,1]$ *reads as* $\max_{-1\le x\le 1}|f(x)-p_2(x)| \le 0.435$.

The real error $\max_{-1\le x\le 1}|f(x)-p_2(x)|$ *is* 0.0785. *Thus, it can be seen that* 0.0785 *is less than* 0.453 *which verifies Theorem 2.2.*

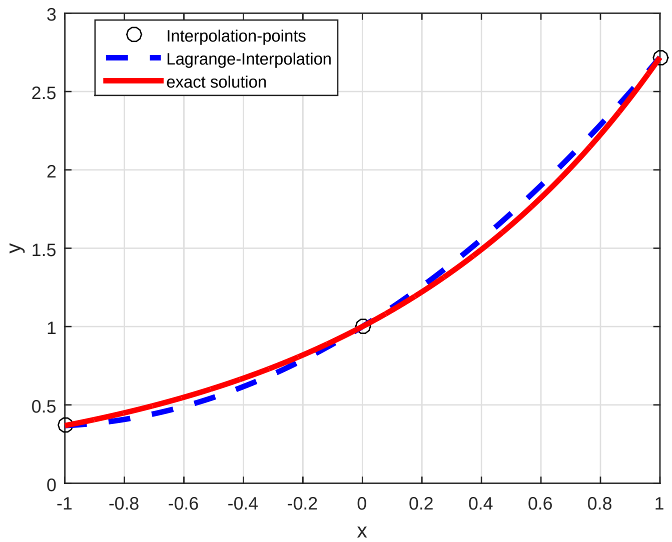

Figure 2.2: Graphs of $f(x) = e^x$ and $p_2(x)$ on $[-1,1]$.

Table 2.1: Maximum error in infinity norm of the difference between $f(x)$ and $p_N(x)$.

N	Maximum error
2	7.85×10^{-2}
3	9.98×10^{-3}
5	1.12×10^{-4}
8	5.80×10^{-8}
10	2.35×10^{-10}
25	7.29×10^{-11}
100	$3.79\times 10^{+11}$

Figure 2.2 presents the graphs of the exponential function $f(x) = e^x$ *and the Lagrange interpolation polynomial of degree* 2 *for* f. *From Figure 2.2, it is observed that the graph of Lagrange interpolation approximates* f *well. Moreover, in Table 2.1, the maximum errors of the difference between the exponential function and Lagrange interpolation polynomial are listed, where it is observed that the error decreases for some values of* N, *whereas when the number of nodes increases, it increases.*

The following example is included to show the existence of the number ζ, which can be unique or not, defined in Theorem 2.2.

Example 2.2. Consider the Lagrange interpolation polynomial of degree 1 *for the following functions:*

i) $f : x \mapsto x^3$ *with interpolation points* $x_0 = 0$ *and* $x_1 = a$.

ii) $f : x \mapsto (2x-a)^4$ *with interpolation points* $x_0 = 0$ *and* $x_1 = a$.

In verifying Theorem 2.2 by direct calculation for both cases, it can be found that:

i) To show that for $f(x) = x^3$, ζ *is unique and* $\zeta = \frac{1}{3}(x+a)$. *We have* $C_0(x) = \frac{x-a}{-a}$, *and* $C_1(x) = \frac{x}{a}$. *The interpolation polynomial is given by* $p_1(x) = C_0(x)f(0) + C_1(x)f(a)$ *which implies that* $p_1(x) = \frac{x-a}{-a}(0)^3 + \frac{x}{a}a^3 = a^2x$. *The following applies*

$$\begin{aligned} f(x) - p_1(x) &= x^3 - a^2x \\ &= x(x^2 - a^2) \\ &= x(x-a)(x+a). \end{aligned} \tag{2.13}$$

By using Theorem 2.2 it is obtained as follows:

$$f(x) - p_1(x) = \frac{f''(\zeta)}{2}x(x-a). \tag{2.14}$$

From (2.13) and (2.14), the following applies: $x(x-a)(x+a) = \frac{f''(\zeta)}{2}x(x-a)$.

It is known that $f''(\zeta) = 6\zeta$. *Therefore,* $x + a = 3\zeta \implies \zeta = \frac{1}{3}(x+a)$.

Hence, there is a unique $\zeta = \frac{1}{3}(x+a)$.

ii) It is seen that $C_0(x) = \frac{x-a}{-a}$, *and* $C_1(x) = \frac{x}{a}$. *Then, the interpolation polynomial is given as:* $p_1(x) = \frac{x-a}{-a}(-a)^4 + \frac{x}{a}a^4 = a^3x - a^3(x-a)$. *The following applies:*

$$\begin{aligned} f(x) - p_1(x) &= (2x-a)^4 + a^3(x-a) - a^3x \\ &= 8x(x-a)(2x^2 - 2ax + a^2). \end{aligned} \tag{2.15}$$

By using Theorem 2.2 it is obtained as:

$$f(x)-p_1(x)=\frac{f''(\zeta)}{2}x(x-a). \tag{2.16}$$

From (2.15) and (2.16), $8x(x-a)(2x^2-2ax+a^2)=\frac{f''(\zeta)}{2}x(x-a)$. *It is known that* $f''(\zeta)=48(2\zeta-a)^2$. *Therefore,* $4(2x^2-2ax+a^2)=12(2\zeta-a)^2$ *which implies that* $\frac{2x^2-2ax+a^2}{12}=\left(\zeta-\frac{a}{2}\right)^2$. *Hence, there are two values of* ζ *given by:* $\zeta=\frac{1}{2}a\pm\left(\frac{2x^2-2ax+a^2}{12}\right)^{\frac{1}{2}}$.

The following theorem known as Weierstrass approximation theorem [10]-[11] shows that any $f\in C[a,b]$ in a given closed interval can be approximated uniformly as close as desired by polynomials.

Theorem 2.3. (*Weierstrass approximation (1885)*)

Suppose that $f\in C[a,b]$, *then given any* $\varepsilon>0$ *there is a polynomial* $p\in\mathscr{P}_N$ *such that*

$$\|f-p\|_\infty\leq\varepsilon. \tag{2.17}$$

This theorem asserts that any continuous real valued function on $[a,b]$, can be approximated to any accuracy by some polynomials. In other words, this theorem says that the polynomials are dense in $C[a,b]$ with respect to the infinity norm. Many different proofs have been found due to the importance of the theorem. The proof given here is proposed by Bernstein in 1912 [12].

Definition 2.2. (*Bernstein's polynomials*)

For each N, a non-negative integer, and $x\in[0,1]$, *the Bernstein polynomials* $B_{Nk}\in\mathscr{P}_N$ *are defined as follows:*

$$B_{Nk}(x)=\frac{N!}{k!(N-k)!}x^k(1-x)^{N-k},\quad k=0,1,\ldots,N. \tag{2.18}$$

The following lemma is included in order to prove Weierstrass approximation theorem by using Bernstein's polynomials which play a central role in Bernstein's proof.

Lemma 2.2. If $f \in C[0,1]$ then,

$$p_N(x) = \sum_{k=0}^{N} B_{Nk}(x) f\left(\frac{k}{N}\right), \quad for \quad 0 \le x \le 1, \tag{2.19}$$

there exists a real number $N = N(\varepsilon)$ such that $\|f - p_N\|_\infty \le \varepsilon$.

Proof. *It is known that $f \in C[0,1]$ which implies the uniform continuity of f on the interval $[0,1]$. Therefore, given $\varepsilon > 0$ there is a $\delta > 0$ such that $|x - k/N| < \delta$ implies that*

$$|f(x) - f(k/N)| < \varepsilon/2 \quad \textit{for all} \quad x \in [0,1]. \tag{2.20}$$

Recall the binomial formula,

$$(x+y)^N = \sum_{k=0}^{N} \frac{N!}{k!(N-k)!} x^k y^{N-k}, \tag{2.21}$$

by setting $y = 1-x$, it is obtained that $\sum_{k=0}^{N} B_{Nk}(x) = 1$. By expanding (2.21), it can be seen that:

$$(1-x+tx)^N = \sum_{k=0}^{N} B_{Nk}(x) t^k, \quad for \quad 0 \le x \le 1. \tag{2.22}$$

The sum $\sum_{k=0}^{N}$ can be written as:

$$\sum_{k=0}^{N} = \sum_{k \in S_1} + \sum_{k \in S_2} \tag{2.23}$$

such that:

$$k \in S_1 \implies \left|x - \frac{k}{N}\right| < \delta, \textit{ and } k \in S_2 \implies \left|x - \frac{k}{N}\right| \ge \delta. \tag{2.24}$$

Differentiating equation (2.22) with respect to t, this gives:

$$Nx(1-x+tx)^{N-1} = \sum_{k=0}^{N} B_{Nk}(x)kt^{k-1}, \quad x \in [0,1]. \tag{2.25}$$

In Equation (2.25), substituting $t = 1$ the following applies:

$$\sum_{k=0}^{N} kB_{Nk}(x) = Nx. \tag{2.26}$$

Differentiating (2.25) with respect to t, this gives:

$$\sum_{k=0}^{N} B_{Nk}(x)k(k-1)t^{k-2} = N(N-1)x^2(1-x+tx)^{N-2}. \tag{2.27}$$

By substituting $t = 1$ from (2.27), it is obtained as:

$$\sum_{k=0}^{N} B_{Nk}(x)k(k-1) = N(N-1)x^2. \tag{2.28}$$

Expanding the expression $\sum_{k=0}^{N} B_{Nk}(x)\left(x-\frac{k}{N}\right)^2$ and using (2.26), and (2.28), the following applies:

$$\begin{aligned}\sum_{k=0}^{N} B_{Nk}(x)\left(x-\frac{k}{N}\right)^2 &= x^2\sum_{k=0}^{N} B_{Nk}(x) - \left(\frac{2x}{N}\right)\sum_{k=0}^{N} kB_{Nk}(x) + \left(\frac{1}{N^2}\right)\sum_{k=0}^{N} k^2 B_{Nk}(x)\\ &= x^2 - \left(\frac{2x}{N}\right)Nx + \left(\frac{1}{N^2}\right)\left[N(N-1)x^2 + Nx\right]\\ &= \frac{x(1-x)}{N}.\end{aligned} \tag{2.29}$$

From (2.18), $B_{Nk} \geq 0$ when $x \in [0,1]$ and $\sum_{k=0}^{N} B_{Nk}(x) = 1$, and using the definition of $p_N(x)$ from (2.19), it is obtained as

$$f(x) - p_N(x) = \sum_{k=0}^{N}\left[f(x) - f\left(\frac{k}{N}\right)B_{Nk}(x)\right]. \tag{2.30}$$

By taking the absolute value of (2.30) and using (2.23), the following applies:

$$\begin{aligned} |f(x)-p_N(x)| &\leq \sum_{k=0}^{N}\left|f(x)-f\left(\frac{k}{N}\right)\right|B_{Nk}(x) \\ &= \sum_{k\in S_1}\left|f(x)-f\left(\frac{k}{N}\right)\right|B_{Nk}(x)+\sum_{k\in S_2}\left|f(x)-f\left(\frac{k}{N}\right)\right|B_{Nk}(x). \end{aligned} \tag{2.31}$$

By using (2.20), the following applies

$$\begin{aligned} \sum_{k\in S_1}\left|f(x)-f\left(\frac{k}{N}\right)\right|B_{Nk}(x) &< \sum_{k\in S_1}\left(\frac{\varepsilon}{2}\right)B_{Nk}(x) \\ &= \left(\frac{\varepsilon}{2}\right)\sum_{k\in S_1}B_{Nk}(x) \\ &= \frac{\varepsilon}{2}. \end{aligned} \tag{2.32}$$

For the other sum, since $f\in C[0,1]$, for all $x\in[0,1]$, there is a $M>0$ such that $|f(x)|<M$. Therefore,

$$\sum_{k\in S_2}\left|f(x)-f\left(\frac{k}{N}\right)\right|B_{Nk}(x)\leq 2M\sum_{k\in S_2}B_{Nk}(x). \tag{2.33}$$

From (2.24), $k\in S_2$ implies that $\left|x-\frac{k}{N}\right|\geq\delta$, and by using equation (2.29) the following inequality is obtained:

$$\delta^2\sum_{k\in S_2}B_{Nk}(x)\leq\sum_{k\in S_2}\left(x-\frac{k}{N}\right)^2B_{Nk}(x)\leq\frac{x(1-x)}{N}. \tag{2.34}$$

From inequality (2.34), the following applies

$$\sum_{k\in S_2}\left(x-\frac{k}{N}\right)^2B_{Nk}(x)\leq\frac{x(1-x)}{\delta^2N}. \tag{2.35}$$

Then,

$$\begin{aligned} \sum_{k\in S_2}\left|f(x)-f\left(\frac{k}{N}\right)\right|B_{Nk}(x) &\leq 2M\sum_{k\in S_2}B_{Nk}(x) \\ &= \frac{2M}{\delta^2}\frac{x(1-x)}{N} \\ &\leq \frac{2M}{\delta^2}\frac{1}{4N} \\ &= \frac{M}{2\delta^2N}, \end{aligned} \tag{2.36}$$

since $0 \le x(1-x) \le \dfrac{1}{4}$ *and all the terms in the sums are positive. Thus, if* $N_0 = \dfrac{M}{2\delta^2\varepsilon}$ *is chosen such that* $N \ge N_0$*, then* $\dfrac{M}{2N\delta^2} < \dfrac{\varepsilon}{2}$*. Therefore,*

$$\sum_{k\in S_2} \left| f(x) - f\left(\frac{k}{N}\right) \right| B_{Nk}(x) \le \frac{\varepsilon}{2}. \tag{2.37}$$

Hence, by adding the two sums (2.32) and (2.37), Equation (2.31) becomes

$$|f(x) - p_N(x)| \le \frac{\varepsilon}{2} + \frac{\varepsilon}{2} = \varepsilon, \tag{2.38}$$

when $N \ge N_0$*. Since the value of* N_0 *does not depend on the value of* x *chosen, the inequality (2.38) holds for all* x *in* $[0,1]$.

□

2.1.1. Convergence

Polynomial interpolants may not behave as the function concerned in every case. They might oscillate much more than the function to be interpolated. In practice, it often happens that when increasing the degree of interpolating polynomial, the error increases. The question that can be asked is whether or not a sequence (p_N) of interpolation polynomials converges to f as N tends to infinity. In fact, the sequence of interpolants might not converge to the function f. A more specific question is required since p_N depends on the distribution of the interpolation points $x_0, x_1, \dots, x_N$, not just on the value of N. A first question which arises is how to derive conditions which imply the convergence of the interpolant. Supposing, for instance, that it is agreed to choose equispaced points on the interval $[a,b]$ with

$$x_j = a + hj, \quad j = 0,1,\dots,N \quad (N \ge 1), \quad h = \frac{b-a}{N}. \tag{2.39}$$

From (2.8), it is seen that p_N depends on x_j and Γ_{N+1}. Thus, the answer regarding the convergence of the sequence of interpolation polynomials p_N relies on the behaviour of Γ_{N+1} as N increases, with $\Gamma_{N+1} = \max_{a\le\zeta\le b} |f^{(N+1)}(\zeta)|$.

In this case $\lim_{N\to\infty} \frac{\Gamma_{N+1}}{(N+1)!} \max_{a\le x\le b} |\omega_{N+1}(x)| = 0$ could be expected, where ω_{N+1} is given in (2.7). Moreover, by using (2.8),

$$\lim_{N\to\infty} \max_{a\le x\le b} |f(x) - p_N(x)| = 0, \tag{2.40}$$

where,

$$\max_{a\le x\le b} |f(x) - p_N(x)| \le \frac{\Gamma_{N+1}}{(N+1)!} \max_{a\le x\le b} |\omega_{N+1}(x)|. \tag{2.41}$$

It is said that (p_N) converges uniformly to f as $N \to \infty$ with equispaced points on the interval $[a,b]$. This gives a sense that the relation (2.40) will be satisfied if all derivatives of f exist and are continuous on $[a,b]$. However, in general, this is not always true since the sequence $(\Gamma_{N+1} \max_{a\le x\le b} |\omega_{N+1}(x)|)$ may tend to infinity as N becomes too large, faster than the sequence $\left(\frac{1}{(N+1)!}\right)$ tends to 0. Therefore, the last factor in the relation (2.41) depends on the choice of the interpolation points. Thus, the useful idea will be to choose the $N+1$ interpolation points in the closed interval $[a,b]$ in such a way that $\max_{a\le x\le b} |\omega_{N+1}(x)|$ does not become too large. The following subsection is included to elaborate on the Runge phenomenon.

2.1.2. Runge Phenomenon

The Runge phenomenon is referred as the problem that can emerge when approaching a function by polynomial interpolation when polynomials of high degree defined on equally spaced points. Runge [13], first observed this phenomenon in 1901, when he was studying the behaviour of the approximation error between a function and its interpolating polynomials. He observed that, there are certain functions for which, when the degree of interpolating polynomials is increased, the interpolation error increases and the corresponding interpolating polynomial oscillates near the boundary of the interpolation interval. This shows that the use of higher degree interpolating polynomial does not always improve accuracy. It is easy to see that the maximum error between the function and the interpolating polynomial depends on the set of interpolation points $\{x_0, x_1, \ldots, x_N\}$. The following example is taken from [10] and illustrates this phenomenon.

Example 2.3. (*Runge's example*)

The function $f : x \mapsto (1+16x^2)^{-1}$ *defined on the interval* $[-1,1]$ *is considered.*

For this example, the maximum error in the infinity norm for equispaced interpolation points on the interval $[-1,1]$ *is checked as well as the convergence behaviour.*

Table 2.2: Maximum error in infinity norm of the difference between $f(x)$ and $p_N(x)$

N	$\|f-p_N\|_\infty$
4	0.3853
10	1.1769
12	1.9692
16	5.9104
20	18.751
50	1.99×10^5
60	4.81×10^7
80	2.95×10^9

Table 2.2 presents the maximum error in the infinity norm of the difference between f *and* p_N *for x in the interval* $[-1,1]$, *for several values of N from* 4 *up to* 80. *It can be observed from the values listed in Table2.2, that the maximum error in the infinity norm of the difference between* f *and* p_N *increases when the number of nodes increases, and then for values from* $N=16$ *up to* $N=80$ *the error becomes too large.*

Figure 2.3 plots the function $f(x)=(1+16x^2)^{-1}$ *and the Lagrange interpolation polynomial* p_4 *for* f *based on equispaced points on the interval* $[-1,1]$. *In this figure, it is observed that* p_4 *tends to approximate reasonably the function* f.

Figure 2.4 presents the function $f(x)=(1+16x^2)^{-1}$ *and the Lagrange interpolation polynomial* p_{12} *for* f *based on equispaced points. From this figure it is observed that* p_{12} *does not seem to approximate* f *closely, and the resulting interpolation oscillates toward the ends of the interval.*

The function f *can be expanded in a power series centered at the origin as follows:* $(1+16x^2)^{-1} = (1-(-16x^2))^{-1} = \sum_{N=0}^{\infty}(-1)^N(-16x^2)^N$.

Hence, $(1+16x^2)^{-1} = \sum_{N=0}^{\infty}(-1)^N(-16)^N x^{2N}$. *The following applies to find the radius of convergence R,* $|-16x^2|<1 \quad \Longrightarrow |x|^2 < \frac{1}{16} \quad \Longrightarrow |x| < \frac{1}{4}$.

Thus, the radius of convergence is $R = \frac{1}{4}$. *The singularities of* f *are at* $1+16z^2 = 0$, *this implies that* $z = \pm\frac{1}{4}i$, *which are the poles of* f *as well. The Taylor series converges therefore only for* $|z| < \frac{1}{4}$. *This is because the complex extension* $(1+16z^2)^{-1}$ *has singularities on the circle* $|z| = \frac{1}{4}$ *so that the infinite series* $\sum_{N=0}^{\infty}(-16)^N z^{2N}$ *has* $R = \frac{1}{4}$. *For points outside the convergence circle, the above infinite power series diverges, including points on the real axis where* $|z| > \frac{1}{4}$. *For the interval* $[-1,1]$, *these poles definitely lie within the region* $\mathscr{C}$, *so that* f *is not analytic in* $\mathscr{C}$. *(A function* $f(z)$ *is said to be analytic in a region* $\mathscr{C}$ *of the complex plane if* $f(z)$ *has a derivative at each point of* $\mathscr{C}$ *[14]). For this reason, convergence on the whole interval* $[-1,1]$ *can not be longer expected.*

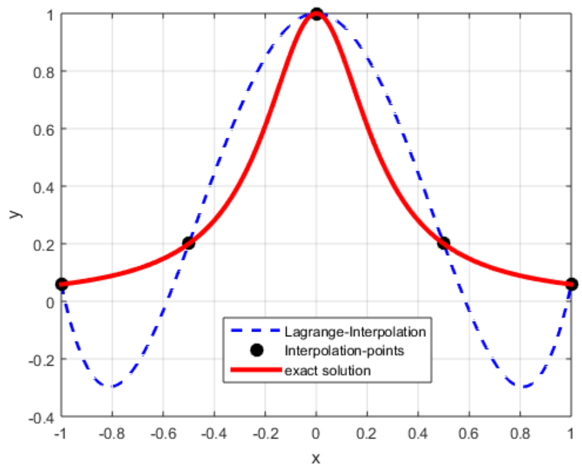

Figure 2.3: Graphs of $f(x) = (1+16x^2)^{-1}$ and $p_N(x)$, for $N = 4$ on $[-1,1]$.

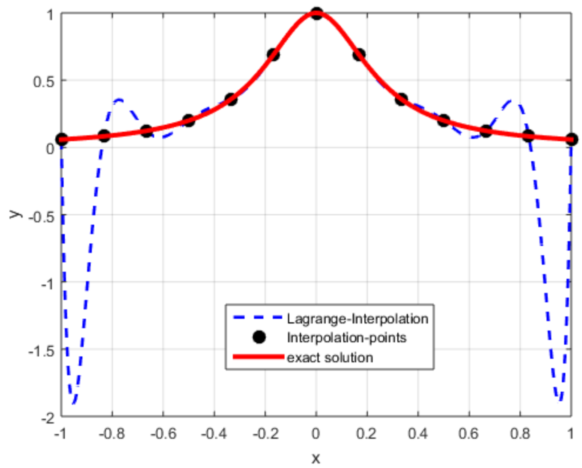

Figure 2.4: Graphs of $f(x) = (1+16x^2)^{-1}$ and $p_N(x)$, for $N = 12$ on $[-1,1]$.

Previously, the notion of Runge phenomenon was discussed. To better understand it was illustrated by an example using equispaced points with interpolating polynomials of degree N. It is observed that for large values of N, the polynomial interpolation of degree N using equispaced points can be troublesome. One of the reasons is that when N increases, the magnitude of the derivatives of Runge's function increases quickly. That is why as it tends to approximate the Runge's function f by polynomial interpolation p_N for higher degree, it is observed that in region close to the end points the maximum error between f and p_N gets larger.

Noting that the Runge phenomenon does not contradict Weierstrass approximation theorem. In the theorem, it is not generalized all the polynomials but only stated the existence of a set of polynomial functions without specifying the case of Lagrange interpolation polynomial at equispaced points. Therefore, the polynomial p_N constructed at equispaced points may diverge away from f as N increases which is the case of Runge phenomenon.

The oscillation observed from the Runge phenomenon toward the end points can be minimized by using CGL points for which, with increasing polynomial order, the maximum error in approximating the Runge function is guaranteed to decrease. In order to better understand this, the following subsection is introduced and the concept of Chebyshev polynomials is provided to minimize approximation error.

Chebyshev polynomials are important in many areas of mathematics and are used in numerical analysis. In the next subsection, some elementary formulae for the manipulation of Chebyshev polynomials are presented and will be used throughout this thesis. The following discussion follows [16]-[17] closely.

2.1.3. Definition Of Chebyshev Polynomials

The Chebyshev polynomial of degree N is denoted $T_N(x)$, and is defined for $x \in [-1,1]$ by the explicit formula

$$T_N(x) = \cos[N \arccos(x)], \quad \text{for all} \quad N \geq 0. \tag{2.42}$$

Note that $T_0(x) = \cos 0 = 1$ and $T_1(x) = \cos(\arccos(x)) = x$. When the first two Chebyshev polynomials $T_0(x)$ and $T_1(x)$ are known, the other polynomials $T_N(x)$ can be obtained by the following recurrence relation: for $N \geq 1$,

$$T_{N+1}(x) = 2xT_N(x) - T_{N-1}(x). \tag{2.43}$$

Lemma 2.3. (*Orthogonality*)

Chebyshev polynomials are orthogonal with respect to the weight function $w(x) = (1-x^2)^{-1/2}$*. That is,*

$$\int_{-1}^{1} T_N(x)T_m(x)(1-x^2)^{-1/2}dx = \begin{cases} 0 & \text{if} \quad m \neq N \\ \frac{\pi}{2} & \text{if} \quad m = N \quad \forall N \geq 1. \end{cases} \tag{2.44}$$

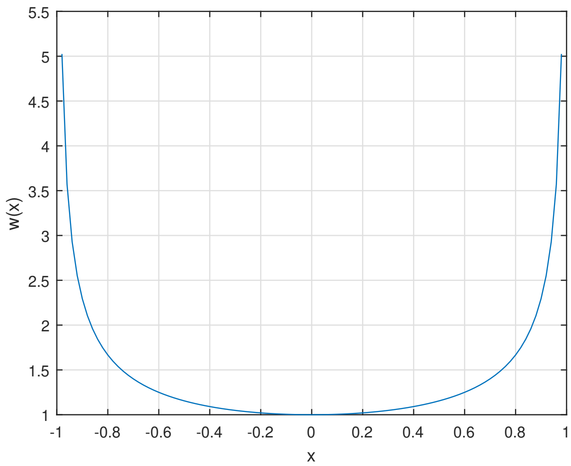

Figure 2.5: Graph of $w(x)$.

$w(x)$ aims to attribute various degrees of importance to approximations on certain parts of the interval.

Figure 2.5 presents the graph of $w(x)$, it is observed that $w(x)$ places more focus close to the endpoints of the interval, and less emphasis close to the center.

The following lemma is included to introduce some properties of Chebyshev polynomials which will be used in this thesis.

Lemma 2.4. The Chebyshev polynomials have the following properties:

i) The coefficient of x^N *in* T_N *is* 2^{N-1} *for* $N \geq 1$.

ii) *For $N = 2m$ (even), then T_{2m} is an even function on $[-1,1]$. This means that $T_{2m}(-x) = T_{2m}(x)$, and when $N = 2m+1$ (odd), then T_{2m+1} is an odd function on $[-1,1]$. This means that $T_{2m+1}(-x) = -T_{2m+1}(x)$ for $N \geq 0$. The symmetry and anti-symmetry of T_{2m} and T_{2m+1} respectively in Figure 2.6 can be seen.*

iii) *For $N \geq 1$, $T_N(x)$ has N real distinct zeros $\bar{x}_k$ which lie in the interval $[-1,1]$. The zeros of T_N are given as follows*

$$\bar{x}_k = \cos\left(\frac{2k-1}{2N}\pi\right), \quad k = 0,1,\ldots,N. \tag{2.45}$$

In this thesis the values of $\bar{x}_k$ are the CG points.

iv) *For $N \geq 0$, the following applies $|T_N(x)| \leq 1$, for $-1 \leq x \leq 1$.*

v) *For $N \geq 1$, $|T_N(x)|$ is maximized on the interval $[-1,1]$ at the $N+1$ points*

$$x_k^{CGL} = \cos\left(\frac{k\pi}{N}\right), \quad k = 0,1,\ldots,N. \tag{2.46}$$

$T_N(x_k^{CGL}) = (-1)^k$, where x_k^{CGL} are the CGL points.

Let $G_N(x) = 2^{1-N} T_N(x)$, and $\mathscr{M}_N$ the set of all monic polynomials of degree N. The following theorem is taken from [17].

Theorem 2.4. The polynomials of the form $G_N(x)$, for $N \geq 1$, have the property that

$$\max_{-1\leq x\leq 1} |Q_N(x)| \geq \max_{-1\leq x\leq 1} |G_N(x)| = 2^{1-N}, \quad for\ all \quad Q_N \in \mathscr{M}_N. \tag{2.47}$$

Furthermore, there is equality if $Q_N \equiv G_N$.

Proof. *Assume that $Q_N \in \mathscr{M}_N$ and that $\max_{-1\leq x\leq 1} |Q_N(x)| \leq \max_{-1\leq x\leq 1} |G_N(x)| = 2^{1-N}$. Let $R = G_N - Q_N$. Then $G_N, Q_N \in \mathscr{M}_N$, therefore, $R \in \mathscr{P}_{N-1}$. Furthermore, at the $N+1$-th CGL points, it is obtained as*

$$R(x_k^{CGL}) = G_N(x_k^{CGL}) - Q_N(x_k^{CGL}) = (-1)^k 2^{1-N} - Q_N(x_k^{CGL}). \tag{2.48}$$

However, for each $k = 0, 1, \ldots, N$, $\quad 2^{1-N} \geq |Q_N(x_k^{CGL})|$. Therefore, for $k = 2m$ (even), $R(x_k^{CGL}) \geq 0$ and $R(x_k^{CGL}) \leq 0$ when $k = 2m+1$ (odd). Since $R \in C[-1,1]$, by using the Intermediate Value Theorem, there is at least one zero of $R(x)$ between x_i^{CGL} and x_{i+1}^{CGL}, for each $i = 0, 1, \ldots, N-1$. Thus, in the interval $[-1,1]$, R has at least N zeros. However $R \in \mathscr{P}_{N-1}$, therefore $R \equiv 0$. Hence $Q_N \equiv G_N$.

□

Recall that in (2.7), it is seen that $\omega_{N+1}(x)$ depends on interpolation points. In order to minimize the interpolation error in (2.7), Theorem 2.4 can be used. Moreover, since $\omega_{N+1}(x) \in \mathscr{M}_{N+1}$, the minimum can be obtained when $\omega_{N+1}(x) = G_{N+1}(x)$. In the case where x_k is considered as the $(k+1)$st zero of G_{N+1}, $\max\limits_{-1\leq x\leq 1} |\omega_{N+1}(x)|$ is the smallest. By choosing x_k to be $\bar{x}_{k+1}$,

$$2^{-N} = \max_{-1\leq x\leq 1} |\omega_{N+1}(\bar{x})| \leq \max_{-1\leq x\leq 1} |\omega_{N+1}(x)|, \tag{2.49}$$

for any choice of interpolation points in $[-1,1]$.

Corollary 2.1. Assume that $p_N \in \mathscr{P}_N$ with points at the zeros of T_{N+1}. Then,

$$\max_{-1\leq x\leq 1} |f(x) - p_N(x)| \leq \frac{2^{-N}}{(N+1)!} \max_{-1\leq x\leq 1} |f^{(N+1)}(x)|, \quad f \in C^{N+1}[-1,1]. \tag{2.50}$$

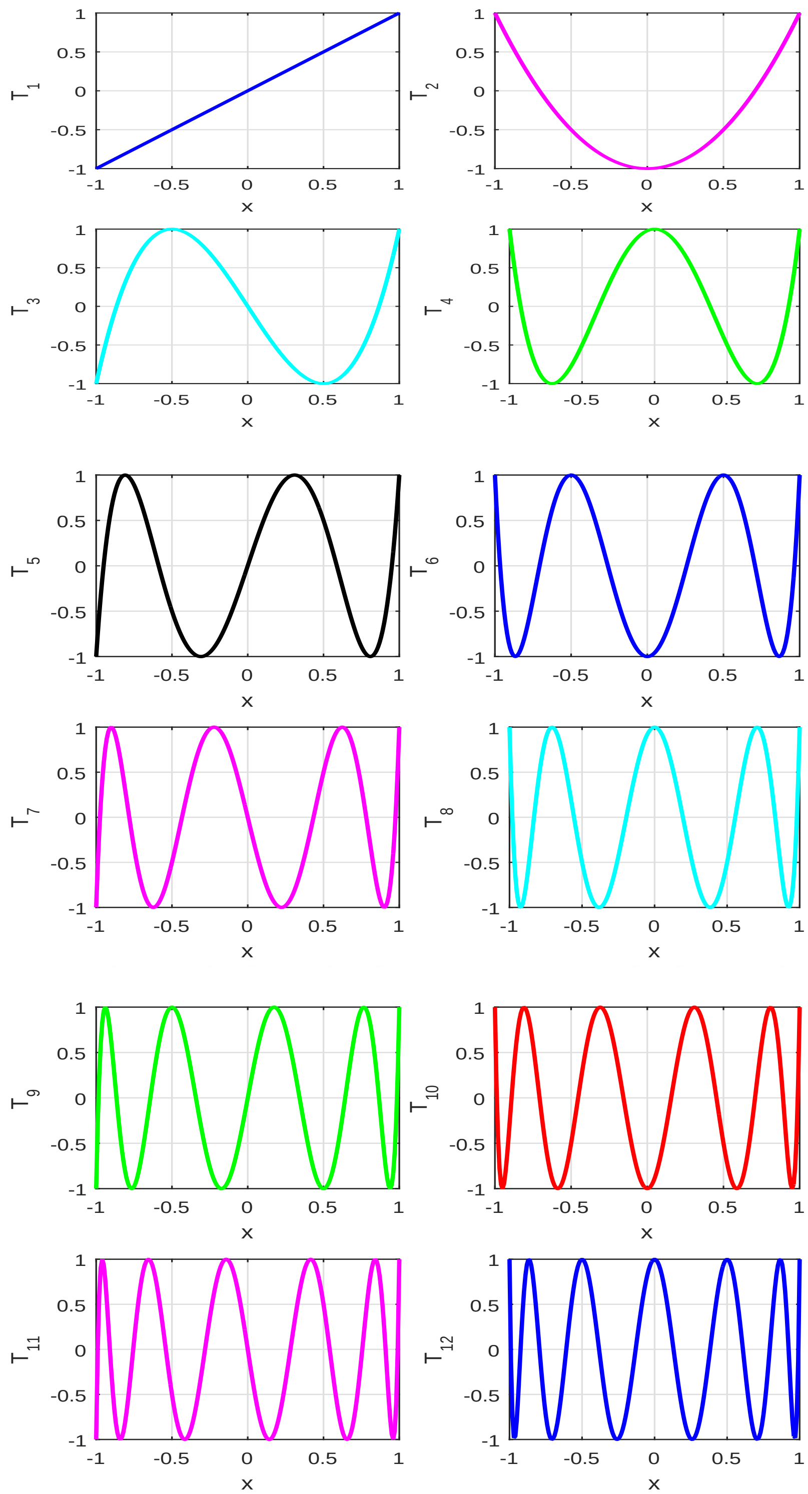

Figure 2.6: Graphs of the first twelve Chebyshev polynomials: $T_1, T_2, \ldots, T_{12}$.

Figure 2.6 presents the graphs of the first twelve Chebyshev polynomials. It is observed that T_N is symmetric according to y-axis when it is an even function, while in the case where T_N is an odd function it is seen that T_N is symmetric according to the origin.

Figure 2.7 presents the CGL points (marked by $*$) as the projections onto the

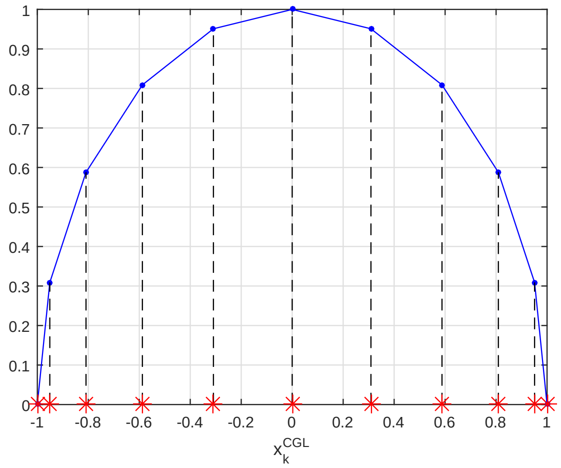

Figure 2.7: Graph of CGL points (marked by $*$) on $[-1,1]$ for $N = 10$.

x-axis of equispaced points on the unit semicircle in the interval $[-1,1]$, and these points are numbered from right to left.

2.2. Polynomial Approximation in The Infinity Norm

In this section, the polynomial approximation in the infinity norm other type of approximation by polynomials is discussed which led to the introduction of the notion of the best approximation in the infinite norm. For better understanding of the best approximation in the infinity norm, the concept of norm is introduced which allows for the quantitative comparison of various approximations after which the polynomial which has the smallest approximation error is selected. To begin with, the following definitions may be recalled.

Definition 2.3. (*Normed linear spaces*).

Let X be a real linear space. A non-negative function $\|.\|$ defined on X is called a norm on X if it satisfies the following axioms:

i) $\|f\| = 0 \quad \Leftrightarrow \quad f = 0$ *in* X.

ii) $\|\alpha f\| = |\alpha|\|f\|, \quad \forall\alpha \in \mathbb{R}, \quad \forall f \in X.$

iii) $\|f_1 + f_2\| \le \|f_1\| + \|f_2\|, \qquad \forall f_1, f_2 \in X.$

$(X, \|.\|)$ *is called a normed linear space.*

Definition 2.4. (∞*-norm*)

The set $C[a,b]$ is a normed linear space with norm:

$$\|f\|_\infty = \max_{x\in[a,b]} |f(x)|. \tag{2.51}$$

The norm $\|.\|_\infty$ is called the infinity norm. For reason to be clear in the sequel, the definition of the 2-norm is included. The 2-norm is defined as

$$\|f\|_2 = \left(\int_a^b |f(x)|^2 w(x)dx\right)^{\frac{1}{2}}, \tag{2.52}$$

where $w(x)$ is an admissible weight function. The following lemma given in [10] (without a proof) provides a comparison between the infinity norm and 2-norm. As it is standard and is very important in the approximation theory highlighting the importance of the working norm, we provide a way to prove it below.

Lemma 2.5. Suppose that $w(x)$ is an admissible weight function on (a,b). Then, for any $f \in C[a,b]$, the following applies $\|f\|_2 \le W\|f\|_\infty$, where $W = \left[\int_a^b w(x)dx\right]^{\frac{1}{2}}$.

For any ε and M positive numbers, there is a $f \in C[a,b]$ such that $\|f\|_2 < \varepsilon$, and $\|f\|_\infty > M$.

Proof.

i) *It is known that $|f(x)| \le \|f\|_\infty = \max_{x\in[a,b]} |f(x)|$. Then, by using (2.52), the following applies*

$$\begin{aligned}\{\|f\|_2\}^2 &= \int_a^b w(x)[f(x)]^2 dx \\ &\le \int_a^b w(x)\|f\|_\infty^2 dx \\ &= \|f\|_\infty^2 \int_a^b w(x)dx.\end{aligned} \tag{2.53}$$

From (2.53), it is obtained as $\{\|f\|_2\}^2 \le W^2\|f\|_\infty^2 \quad \Longrightarrow \|f\|_2 \le W\|f\|_\infty$.

ii) *For the given M, defining f such that $\|f\|_\infty = \alpha M$ with $\alpha \ge 1$, so $\|f\|_\infty = \alpha M > M$.*

Choosing $f(x)$ such that: $f(x) = \begin{cases} -\frac{\alpha M}{\delta}(x-a-\delta) & \text{if} \quad a \le x \le a+\delta \\ 0 & \text{if} \quad a+\delta \le x \le b. \end{cases}$

Then, $w(x) = 1$.

$$\begin{aligned} \{\|f\|_2\}^2 &= \int_a^b \left| \frac{\alpha M}{\delta}(x-a-\delta) \right|^2 dx \\ &= \frac{\alpha^2 M^2}{\delta^2} \int_a^{a+\delta} (x-a-\delta)^2 dx \\ &= \frac{\alpha^2 M^2}{\delta^2} \frac{(x-a-\delta)^3}{3} \bigg|_a^{a+\delta} \\ \{\|f\|_2\}^2 &= \frac{\alpha^2 M^2 \delta}{3}. \end{aligned} \tag{2.54}$$

From (2.54), it is obtained as $\|f\|_2 = \alpha M \sqrt{\frac{\delta}{3}}$.

If δ is chosen such that $\|f\|_2 = \alpha M \sqrt{\frac{\delta}{3}} < \varepsilon$, then $\|f\|_2 < \varepsilon$. Therefore, when $\alpha > 1$ and $\delta < \dfrac{3\varepsilon^2}{\alpha^2 M^2}$ satisfies $\|f\|_2 < \varepsilon$, and $\|f\|_\infty > M$, for any positive numbers ε and M.

□

The following subsection investigates the polynomial p_N of degree at most N that best approximates $f \in C[a,b]$ uniformly on $[a,b]$. For this, the infimum of the distance between f and all possible degree at most N polynomial approximations is sought. The theorems presented in the following subsection are proved in [10] and adapted for completeness.

2.2.1. Best Approximation Of Degree N in Infinity Norm

Given that $f \in C[a,b]$, and N a positive integer. The problem is to find $p_N \in \mathscr{P}_N$, such that $\|f - p_N\|_\infty = \inf_{q \in \mathscr{P}_N} \|f - q\|_\infty, \quad \forall q \in \mathscr{P}_N$.

It is known that such a polynomial exists uniquely and it is called as the minimax polynomial [10].

The following theorem is included to provide a characterization of the oscillation property of the minimax polynomial.

Theorem 2.5. (*The Oscillation Theorem*)

Let $f \in C[a,b]$. A polynomial $r \in \mathscr{P}_N$ is a minimax polynomial for f on $[a,b]$ if, and only if, there is a sequence of $N+2$ points such that $a \le x_0 < \cdots < x_{N+1} \le b$,

$$|f(x_i) - r(x_i)| = \|f - r\|_\infty, \; for \; i = 0, 1, \ldots, N+1, \tag{2.55}$$

and

$$f(x_i) - r(x_i) = -[f(x_{i+1}) - r(x_{i+1})], \; for \; i = 0, 1, \ldots, N. \tag{2.56}$$

The following example is included to illustrate how to construct the minimax polynomial for the exponential function on the interval $[1,3]$.

Example 2.4. The function $f(x) = e^x$ defined on $[1,3]$ is considered. From this, the minimax approximation polynomial $q_1 \in \mathscr{P}_1$ of degree 1 to f on $[1,3]$ is constructed.

Let $u_1(x)$ be the line which connects the endpoints $(1, f(1))$ and $(3, f(3))$, this means that,

$$u_1(x) = e + \left(\frac{e^3 - e}{3-1}\right)(x-1) = e + \left(\frac{e^3 - e}{2}\right)(x-1). \tag{2.57}$$

From (2.57), it is obtained as: $u_1(x) = e + s(x-1)$, where $s = \dfrac{e^3 - e}{2}$ is the slope. Hence, $u_1(x) = 8.6836x - 5.9653$.

Now, the minimax polynomial $q_1(x) = \beta_1 x + \beta_0$ can be sought for, such that q_1 and f have an alternating set $\{1,\ \alpha,\ 3\}$. Let E_m be the difference between f and q_1 in infinity norm. The Oscillation theorem asserts that if q_1 is a minimax polynomial to f, then there exist $N+2$ points in $[1,3]$ on which the error $f - q_1$ changes sign. In our case $N = 1$, therefore, the maximum error E_m is attained at three points which are 1, 3, and $\alpha \in (1,3)$ to be determined, that attains the same maximal error E_m with opposite sign. The following three equations may be considered:

$$f(1) - q_1(1) = e - \beta_0 - \beta_1 = E_m \tag{2.58}$$

$$f(\alpha) - q_1(\alpha) = e^\alpha - \beta_0 - \beta_1 \alpha = -E_m \tag{2.59}$$

$$f(3) - q_1(3) = e^3 - \beta_0 - 3\beta_1 = E_m. \tag{2.60}$$

There are four unknowns $(\beta_0, \beta_1, \alpha, E_m)$ *and three equations, a fourth equation is obtained by requiring that the error has a maximum at* $x = \alpha$ *when* $f'(\alpha) - q_1'(\alpha) = 0$. *This gives:*

$$e^{\alpha} - \beta_1 = 0. \tag{2.61}$$

Subtracting (2.60) from (2.58) to eliminate E_m *and obtain* β_1.

Then, $e^3 - \beta_0 - 3\beta_1 - e + \beta_0 + \beta_1 = 0 \implies e^3 - e - 2\beta_1 = 0 \implies \beta_1 = \dfrac{e^3 - e}{2}$ $\implies \beta_1 \approx 8.6836$.

From (2.61), it is obtained as: $e^{\alpha} = \beta_1 \implies \alpha = \log \beta_1$. *This gives,* $\alpha \approx 2.1614$.

Adding (2.59) from (2.58) to eliminate E_m *and obtain* β_0.

Then, $e - \beta_0 - \beta_1\alpha + e - \beta_0 - \beta_1 = 0 \implies -2\beta_0 + e^{\alpha} - \beta_1(1+\alpha) = 0$ $\implies \beta_0 = \dfrac{1}{2}(e^{\alpha} + e - \beta_1(1+\alpha)) \implies \beta_0 \approx -8.0254$.

Hence, the minimax polynomial $q_1(x)$ *is given by:*

$$q_1(x) = 8.6836x - 8.0254. \tag{2.62}$$

The maximum error is given by: $\|E_m\|_\infty = \|f - q_1\|_\infty = 2.0601$.

Let $u_2(x)$ *be the tangent to* $f(x)$ *at a point* α, *the following applies*

$$u_2(x) = f(\alpha) + f'(\alpha)(x - \alpha) = \beta_1 + \beta_1(x - \alpha) = \beta_1 x + \beta_1(1 - \alpha). \tag{2.63}$$

Hence, from (2.63), it is obtained as: $u_2(x) = 8.6836x - 10.0855$.

Figure 2.8 presents the graphs of the exponential function (continuous curve), the minimax polynomial q_1 *of degree* 1 *for* f *(straight line), the line* u_1 *(the dotted curve), and the tangent* u_2 *(the dotted curve). By observing Figure 2.8, it can be seen that the line* u_1 *and the tangent* u_2 *are parallel and the graph of the approximation polynomial* q_1 *is parallel to these two lines, and it lies at equal distance between them.*

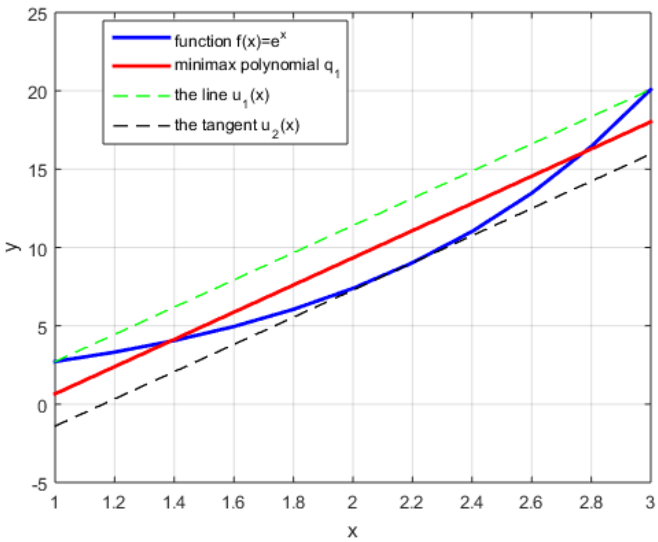

Figure 2.8: Graphs of $f(x) = e^x$ and $q_1(x)$ the minimax polynomial of degree 1 for f on $[1,3]$.

Another example follows to illustrate the construction of the minimax polynomial for the function x^2 on the interval $[0,2]$.

Example 2.5. The function $f(x) = x^2$ defined on the interval $[0,2]$ is considered. From this the minimax approximation polynomial $q_1 \in \mathscr{P}_1$ of degree 1 to f on $[0,2]$ is constructed.

Assume that the minimax polynomial $q_1 \in \mathscr{P}_1$ has the form $q_1(x) = \beta_1 x + \beta_0$. A straight line $q_1(x) = \beta_1 x + \beta_0$ can be sought for, such that q_1 and f have an alternating set $\{0,\ \alpha,\ 2\}$. Let E_m be the maximum error $\|f - q_1\|_\infty$. According to the Oscillation theorem if q_1 is a minimax polynomial to f, then there exist $N+2$ points in $[0,2]$ on which the error $f - q_1$ changes sign. In this case $N = 1$, therefore, the maximum error E_m is attained at three points which are 0, 2, and $\alpha \in (0,2)$ to be determined, that attains the same maximal error E_m with opposite sign. The following three equations may be considered:

$$f(0) - q_1(0) = -\beta_0 = E_m \tag{2.64}$$

$$f(\alpha) - q_1(\alpha) = \alpha^2 - \beta_0 - \beta_1\alpha = -E_m \tag{2.65}$$

$$f(2) - q_1(2) = 4 - \beta_0 - 2\beta_1 = E_m. \tag{2.66}$$

There are four unknowns $(\beta_0, \beta_1, \alpha, E_m)$ and three equations, a fourth equation is obtained by requiring that the error has a maximum at $x = \alpha$ when $f'(\alpha) - q_1'(\alpha) = 0$ yields. This gives:

$$2\alpha - \beta_1 = 0. \tag{2.67}$$

Subtracting (2.66) from (2.64) to eliminate E_m and obtain β_1.

Then, $4 - \beta_0 - 2\beta_1 + \beta_0 = 0 \implies 2\beta_1 = 4 \implies \beta_1 = 2.$

From (2.67) then, $2\alpha = \beta_1 \implies \alpha = \dfrac{\beta_1}{2}$*. This gives,* $\alpha = 1$*. Adding (2.65) from (2.64) to eliminate E_m and obtain β_0.*

Then, $\alpha^2 - \beta_0 - \beta_1\alpha - \beta_0 = 0 \implies -2\beta_0 + \alpha^2 - \beta_1\alpha = 0 \implies \beta_0 = \dfrac{1}{2}\left(\alpha^2 - \beta_1\alpha\right)$
$\implies \beta_0 = -\dfrac{1}{2}.$

Hence, the minimax polynomial $q_1(x)$ is given by:

$$q_1(x) = 2x - \frac{1}{2}. \tag{2.68}$$

The maximum error is given by:

$$\|E_m\|_\infty = \|f - q_1\|_\infty = 0.5. \tag{2.69}$$

Let $u_1(x)$ be the line which connects the endpoints $(0, f(0))$ and $(2, f(2))$, this means that,

$$u_1(x) = f(0) + \left(\frac{f(1) - f(0)}{2 - 0}\right)(x - 0) = 0 + \left(\frac{4}{2}\right)x. \tag{2.70}$$

From (2.70), it is obtained as $u_1(x) = 2x$.

Let $u_2(x)$ be the tangent to $f(x)$ at a point α which is given by:

$$u_2(x) = f(\alpha) + f'(\alpha)(x - \alpha) = 1 + 2(x - \alpha). \tag{2.71}$$

Hence, from (2.71), it is obtained as $u_2(x) = 2x - 1$.

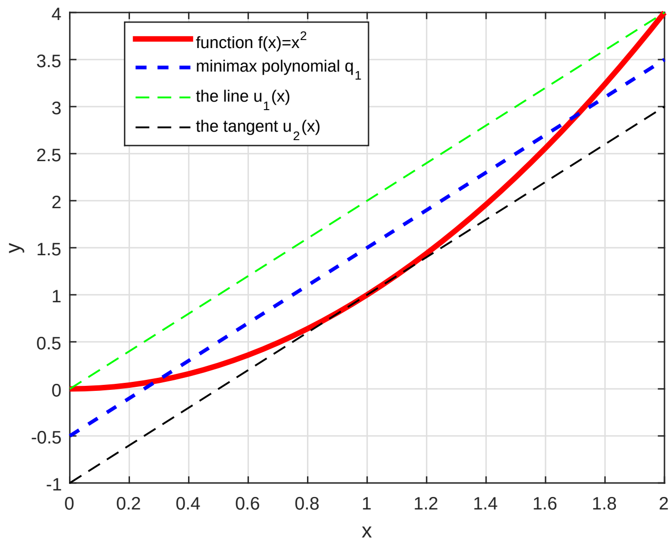

Figure 2.9: Graphs of $f(x) = x^2$ and $q_1(x)$ the minimax polynomial of degree 1 for f on $[0,2]$.

Figure 2.9 presents the graphs of the function $f(x) = x^2$ (continuous curve), the minimax polynomial q_1 of degree 1 *for f (straight line) parallel between u_1 and u_2, the line u_1 (the dotted curve), and the tangent u_2 (the dotted curve). From Figure2.9, it is observed that the minimax approximation polynomial q_1 is the straight line and the curve graph is the plot of the function x^2 and then the maximum error between f and q_1 is* 0.5.

The following subsection introduces the Lebesgue function and its maximum over the domain of interpolation polynomial. Furthermore, three sets of points, namely equispaced points, CG points and CGL points are investigated in terms of Lebesgue constant to determine their interpolation properties.

2.2.2. The Lebesgue Function And The Lebesgue Constant

The Lebesgue function is defined as the summation of the absolute value of Lagrange basis functions. The Lebesgue constant which is the maximum of the Lebesgue function, depends on the interpolation points and gives an idea on the closeness of Lagrange interpolation polynomial p_N to the best approximation polynomial of degree N. One of the reasons for investigating the Lebesgue constant is related to the upper bound in the interpolation error $\|f - p_N\|_\infty$, which will be shown later in this subsection.

The operator that associates the spaces of continuous functions and polynomials $\mathscr{P}_N$ is linear and it is given as

$$P_N : C[a,b] \;\rightarrow\; \mathscr{P}_N : f(x) \;\rightarrow\; p_N; \quad p(.) = p_N(f;.). \tag{2.72}$$

Therefore, for $\alpha_1, \alpha_2 \in \mathbb{R}$, and $f_1, f_2 \in C[a,b]$ then $P_N(\alpha_1 f_1 + \alpha_2 f_2) = \alpha_1 P_N f_1 + \alpha_2 P_N f_2$. Furthermore, for all $f \in \mathscr{P}_N$, $P_N f = f$ which implies that P_N is a projection operator [18]. A norm of P_N can be defined as follows:

$$\|P_N\| = \max_{\substack{f\in C[a,b]\\ f\neq 0}} \frac{\|P_N f\|}{\|f\|}. \tag{2.73}$$

Taking the infinity norm of the Lagrange interpolating polynomial of f associated with the interpolation points given in (2.6), it is obtained [18]

$$\begin{aligned} \|p_N(f;.)\|_\infty &= \max_{a\leq x\leq b} |\sum_{k=0}^{N} f(x_k) C_k(x)| \\ &\leq \|f\|_\infty \max_{a\leq x\leq b} \sum_{k=0}^{N} |C_k(x)| \\ &= \|f\|_\infty \|\lambda_N\|_\infty, \end{aligned} \tag{2.74}$$

where

$$\lambda_N(x) = \sum_{k=0}^{N} |C_k(x)| \tag{2.75}$$

is called the Lebesgue function. Define,

$$\Lambda_N = \max_{a\leq x\leq b} (\lambda_N(x)) \tag{2.76}$$

as the Lebesgue constant. It is clear that $\lambda_N(x)$ and Λ_N depend on the interpolation points but not on the function $f(x_k)$. Thus, the Lebesgue constant is a numerical value which provides a measure of the interpolation error compared to the best polynomial approximation in the infinity norm.

Let q_N be the best approximation of f on $[a,b]$ in the infinity norm by polynomials of degree at most N. By using the projection property $P_N q_N = q_N$, and (2.74)-(2.76), it is obtained that,

$$\begin{aligned}
\|f - p_N f\|_\infty &= \|f - q_N + q_N - p_N f\|_\infty \\
&\leq \|f - q_N\|_\infty + \|q_N - p_N f\|_\infty \\
&= \|f - q_N\|_\infty + \|p_N(q_N - f)\|_\infty \\
&\leq \|f - q_N\|_\infty + \Lambda_N \|f - q_N\|_\infty \\
&\leq (1 + \Lambda_N)\|f - q_N\|_\infty .
\end{aligned} \tag{2.77}$$

Hence, p_N converges to f as the factor $\Lambda_N \|f - q_N\|_\infty$ goes to 0 as N tends to infinity. However, Λ_N is not uniformly bounded.

In order to have a good approximation, we would like to choose the interpolation points in such a way that Λ_N does not become too large. The following theorem is taken from [19] which asserts the existence of a positive constant c such that no matter how the points $x_0, x_1, \ldots, x_N$ are chosen, $\Lambda_N > O(\log N)$ always holds as $N \to \infty$.

Theorem 2.6. For any sequence of interpolation points, there exists a positive constant c such that

$$\Lambda_N > \frac{2}{\pi} \log(N+1) - c. \tag{2.78}$$

In order to answer the question about the best choice of interpolating points, firstly, the attention is focused on the case of equispaced points with the associated Lebesgue constant denoted by Λ_N^{Eqs}, and then discussion on the case of CG points which are Chebyshev points of the first kind with the associated Lebesgue constant Λ_N^{CG} is provided. And further discussions on the case of CGL points (extreme points) with the associated Lebesgue constant Λ_N^{CGL} are presented. And finally, a comparison of the three cases to see which one is more accurate than the other is also carried out.

Starting with the case of equispaced points, the following theorem taken from [20] which gives the upper and lower bounds of Λ_N^{Eqs} is included.

Theorem 2.7. For each integer $N \geq 1$, the Lebesgue constant Λ_N^{Eqs} is bounded as:

$$\frac{2^{N-2}}{N^2} < \Lambda_N^{Eqs} < \frac{2^{N+3}}{N} \tag{2.79}$$

with the asymptotic estimate

$$\Lambda_N^{Eqs} \approx \frac{2^{N+1}}{eN(\log N+\gamma)}, \quad N \to \infty \tag{2.80}$$

where $\gamma = 0.57721566$ *is the constant known as Euler's constant.*

From relation (2.80), it is observed that the Lebesgue constant Λ_N^{Eqs} grows fastly when N increases. This shows that when the number of nodes increases, interpolation using equispaced points results in a very poor approximation. Therefore, the choice of equispaced points results in an inconvenient interpolation in connection with the Runge phenomenon. Figure 2.10 and Table 2.3 are included to better illustrate a result of choosing equispaced points for the polynomial interpolation.

Table 2.3: Lebesgue constant Λ_N^{Eqs} for equispaced points.

N	Λ_N^{Eqs}
1	1
2	1.25
3	1.6311
4	2.2078
5	3.1063
10	29.8981
15	512.34
20	1.0979×10^4
65	8.8449×10^{16}
100	1.7575×10^{27}

From Table 2.3 it can be seen that the Lebesgue constant Λ_N^{Eqs} increases dramatically as N increases.

In Figure 2.10, the graphs of the Lebesgue function for $N = 5, 10, 15, 20$ using equispaced points are drawn, where it is observed that the Lebesgue function oscillates near the endpoints as in case of Runge phenomenon. It is also seen that near the midpoint of the interval $[-1, 1]$ the Lebesgue function decreases. Furthermore, when the number of nodes increases, interpolation using equispaced points results in a very poor

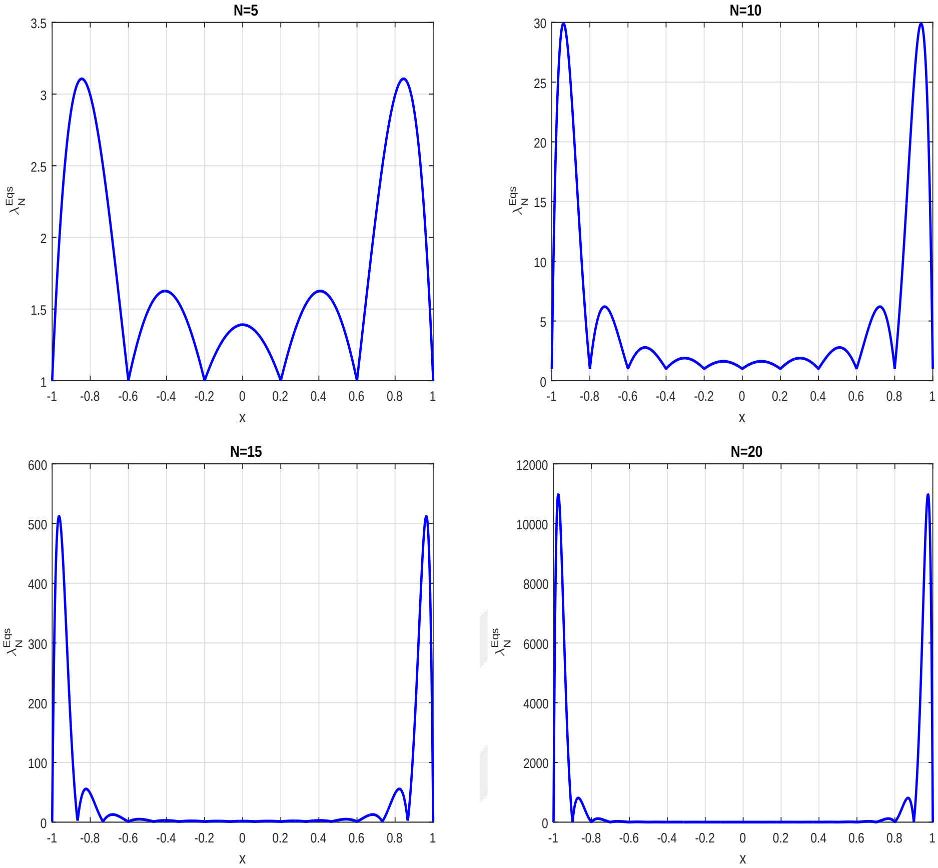

Figure 2.10: Graphs of Lebesgue function λ_N^{Eqs}, for $N = 5, 10, 15, 20$.

approximation. It can be seen that the Lebesgue constant Λ_N^{Eqs} of equispaced points increases very fast when N increases.

The case of CG points defined in (2.45) which are the zeros of Chebyshev polynomials T_N is considered next. In [21] the Lebesgue constant for interpolation using the CG points denoted by Λ_N^{CG} is given as:

$$\Lambda_N^{CG} = \frac{2}{\pi}\left(\log N + \gamma + \log\frac{8}{\pi}\right) + \alpha_N, \text{ where } 0 < \alpha_N < \frac{\pi}{72(N+1)^2}, \; N \geq 1. \quad (2.81)$$

Table 2.4 presents the Lebesgue constant for CG points for various N. It can be seen that the Lebesgue constant Λ_N^{CG} is not too large when N increases compared to the case of equispaced points. Figure 2.11 presents the graphs of the Lebesgue function for $N = 5, 10, 15, 20$, using CG points. From this figure it is seen that when the number of nodes increases, interpolation using CG points results in a good approximation.

Table 2.4: Lebesgue constant Λ_N^{CG} for CG points.

N	Λ_N^{CG}
1	1.4142
2	1.6667
3	1.8478
4	1.9889
5	2.1044
10	2.4894
15	2.7278
20	2.9008
65	3.6297
100	3.9006

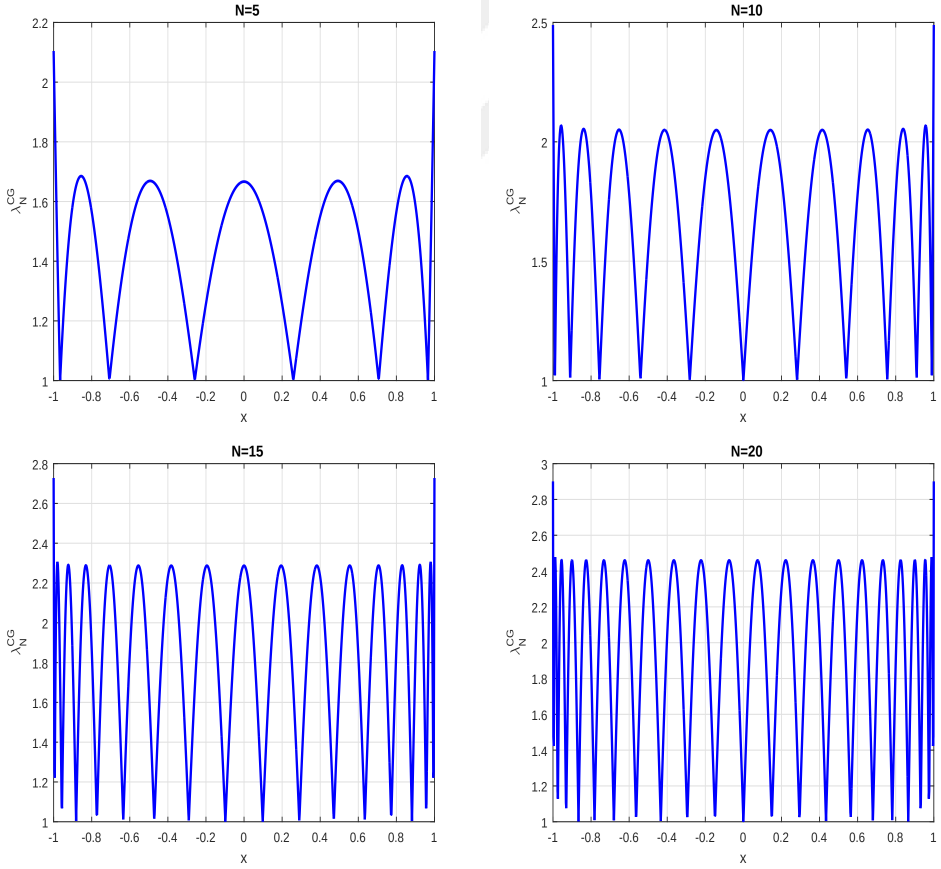

Figure 2.11: Graphs of Lebesgue function λ_N^{CG}, for $N = 5, 10, 15, 20$.

The case of CGL points with the associated Lebesgue constant Λ_N^{CGL} is finally presented. Recall that the CGL points are the zeros of the polynomial $(1-x^2)T_N'(x)$

and are defined in (2.46) which are the extrema points of Chebyshev polynomials of $T_N(x)$ over $[-1,1]$.
In [22] the Lebesgue constant for interpolation using CGL points Λ_N^{CGL} is given as:

$$\Lambda_N^{CGL} = \frac{2}{\pi}\left(\log N + \gamma + \log\frac{8}{\pi}\right) + O\left(\frac{1}{N^2}\right), \tag{2.82}$$

where N is the number of points and γ is the Euler's constant.

Table 2.5: Lebesgue constant Λ_N^{CGL} for CGL points.

N	Λ_N^{CGL}
1	1
2	1.25
3	1.6667
4	1.7988
5	1.9889
10	2.4210
15	2.6867
20	2.8677
65	3.6200
100	3.8930

Table 2.5 is included to better understand why the choice of CGL points for the polynomial interpolation is more accurate than equispaced points.

Table 2.5 presents Lebesgue constant for CGL points for various N, where it can be seen that the values of Λ_N^{CGL} are not too large when N increases compared to the two other cases, namely equispaced points and CG points.

Figure 2.12 presents the graphs of the Lebesgue function for $N = 5, 10, 15, 20$, using CGL points. From this figure it is seen that when the number of nodes increases, interpolation using CGL points results in a good approximation.

In order to better understand the choice of interpolating points and to allow a comparison in terms of accuracy Λ_N^{Eqs}, Λ_N^{CG}, and Λ_N^{CGL} are compared in Table 2.6.

By comparing Λ_N^{Eqs}, Λ_N^{CG}, and Λ_N^{CGL} listed in Table 2.6, it can be observed that

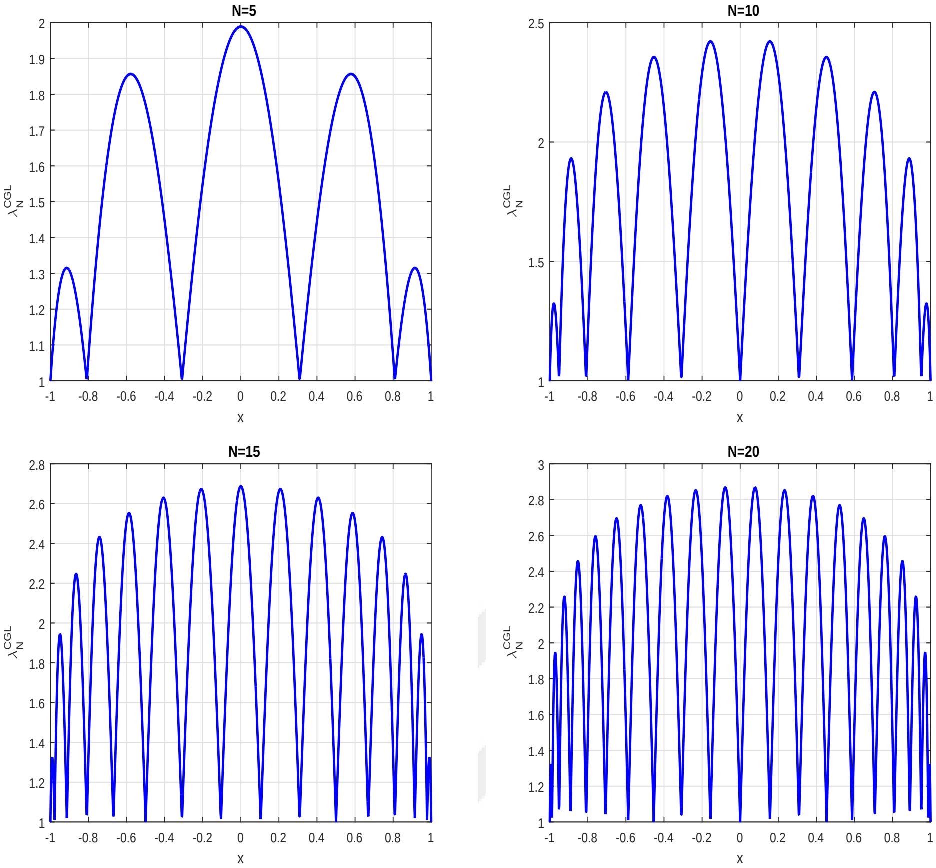

Figure 2.12: Graphs of Lebesgue function λ_N^{CGL}, for $N = 5, 10, 15, 20$.

Table 2.6: Comparison between Λ_N^{Eqs}, Λ_N^{CG}, and Λ_N^{CGL}.

N	Λ_N^{Eqs}	Λ_N^{CG}	Λ_N^{CGL}
1	1	1.4142	1
2	1.25	1.6667	1.25
3	1.6311	1.8478	1.6667
4	2.2078	1.9889	1.7988
5	3.1063	2.1044	1.9889
10	29.8981	2.4894	2.4210
15	512.34	2.7278	2.6867
20	1.0979×10^4	2.9008	2.8677
65	8.8449×10^{16}	3.6297	3.6200
100	1.7575×10^{27}	3.9006	3.8930

the CGL points yield the smallest Lebesgue constants among the three interpolation points. It can also be seen that Λ_N^{Eqs} of equispaced points increases very fast when N

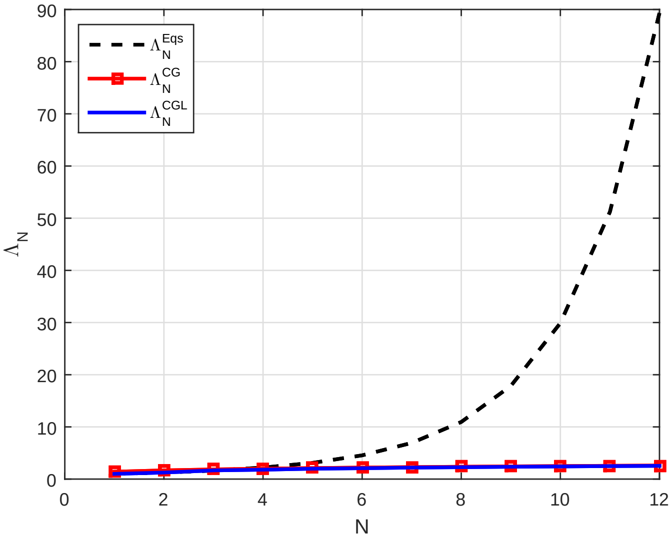

Figure 2.13: Variation of Λ_N^{Eqs}, Λ_N^{CG}, and Λ_N^{CGL}, with respect to N.

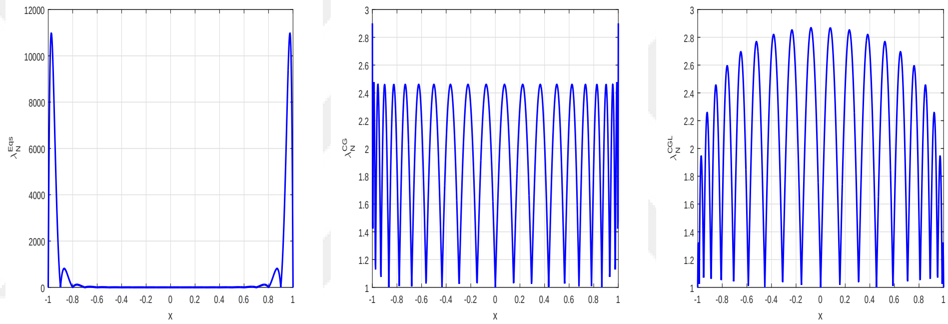

Figure 2.14: Graphs of Lebesgue function λ_N^{Eqs} (left), λ_N^{CG} (middle), and λ_N^{CGL} (right), for $N = 20$.

increases.

Figure 2.13 presents the plots for Λ_N^{Eqs}, Λ_N^{CG}, and Λ_N^{CGL} for varying N. Figure 2.14 presents the plots for Lebesgue function λ_N^{Eqs}, λ_N^{CG}, and λ_N^{CGL} for $N = 20$. By observing Figure 2.13 it can also be seen that when N increases Λ_N^{Eqs} of equispaced points increases very fastly. From Figure 2.13 and Figure 2.14 it is observed that the CGL points are the most accurate among the three sets of interpolation points.

Figure 2.15 presents the plot for Lebesgue constant Λ_N^{CGL} for varying N. From this figure it is observed that even for a large value as $N = 500$, the Lebesgue constant in the case of CGL points is not very large compared to that of equispaced points for $N = 12$.

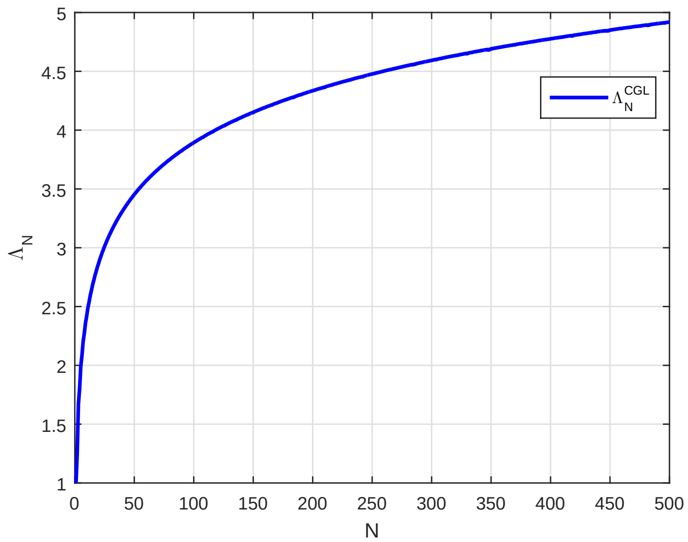

Figure 2.15: Graph of variation of Lebesgue constant Λ_N^{CGL}, with respect to $N = 500$.

In addition, by using the inequality (2.77) for $N = 200$, the interpolation error based on the equispaced points is computed as

$$\|f - p_N\|_\infty \leq (9.63 \times 10^{56})\|f - q_N\|_\infty. \tag{2.83}$$

The case of the interpolation error based on the CG points for the same degree can be considered as follows:

$$\|f - p_N\|_\infty \leq (5.34 \times 10^{0})\|f - q_N\|_\infty. \tag{2.84}$$

For comparison if CGL points for the same N are chosen, then the interpolation error is:

$$\|f - p_N\|_\infty \leq (5.33 \times 10^{0})\|f - q_N\|_\infty. \tag{2.85}$$

From (2.83)-(2.85), it is concluded that the choice of CGL points is more accurate than other two interpolating points.

In the following example which is taken from [15] the maximum error in the infinity norm for equispaced and CGL interpolation points on the interval $[-1, 1]$ as well as the convergence behaviour are investigated.

Example 2.6. (*Runge's example*)

The function $f : x \mapsto (1+16x^2)^{-1}$ *which is considered by using equally spaced interpolation is now considered with CGL points defined on the interval* $[-1,1]$.

Table 2.7: Comparison of the maximum error in the infinity norm of the difference between f and; each of p_N and $\tilde{p}_N$ with equispaced ($\|f-p_N\|_\infty$) and CGL points ($\|f-\tilde{p}_N\|_\infty$).

N	$\|f-p_N\|_\infty$	$\|f-\tilde{p}_N\|_\infty$
4	0.3853	0.37083
10	1.1769	0.07476
12	1.9692	0.04251
16	5.9104	0.01754
20	18.751	6.67×10^{-3}
50	1.99×10^{5}	3.96×10^{-6}
60	4.81×10^{7}	3.35×10^{-7}
80	2.95×10^{9}	2.36×10^{-9}

Table 2.7 presents the maximum error in the infinity norm of the difference between f *and; each of* p_N, *and* $\tilde{p}_N$ *for* x *in the interval* $[-1,1]$ *using equispaced and CGL points respectively, for several values of* N *from* 4 *up to* 80. *From Table 2.7, it is observed that the maximum error in the infinity norm of the difference between* f *and* p_N *increases when the number of nodes increases, and then for values from* $N=16$ *up to* 80 *the error becomes too large (Runge phenomenon) as previously explained, while the maximum error in the infinity norm of the difference between* f *and* $\tilde{p}_N$ *decreases when* N *increases.*

Figure 2.16 plots the function $f(x)=(1+16x^2)^{-1}$ *and the Lagrange interpolation polynomial* p_{10} *for* f *based on equispaced points on the interval* $[-1,1]$. *From this figure it is observed that the graph of the Lagrange interpolation polynomial* p_{10} *does not seem to approximate* f, *and the resulting interpolation oscillates toward the ends of the interval* $[-1,1]$.

Figure 2.17 presents the function $f(x)=(1+16x^2)^{-1}$ *and the Lagrange interpolation polynomial* p_{10} *for* f *based on CGL points on the interval* $[-1,1]$. *From this figure it can be seen that the graph of the Lagrange interpolation* p_{10} *approximates the*

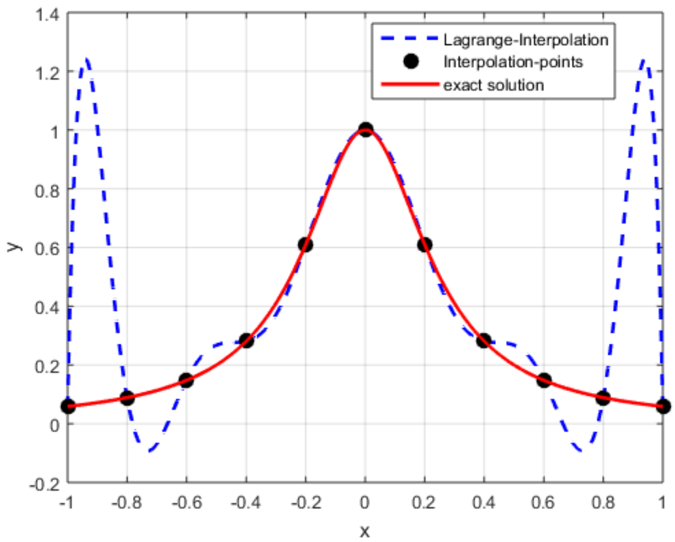

Figure 2.16: Graphs of $f(x) = (1+16x^2)^{-1}$ and its polynomial interpolation $p_N(x)$ with equispaced points for $N = 10$ on $[-1,1]$.

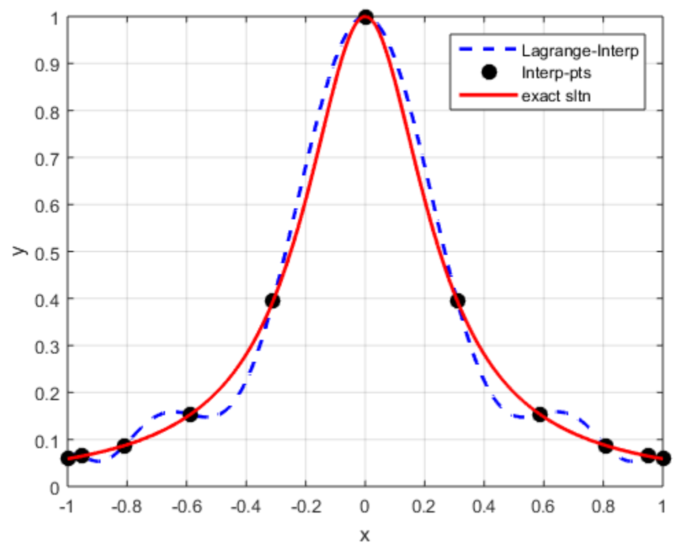

Figure 2.17: Graphs of $f(x) = (1+16x^2)^{-1}$ and its polynomial interpolation $p_N(x)$ with CGL points for $N = 10$ on $[-1,1]$.

function f well.

Figure 2.18 presents the graphs of the absolute errors of the function f and its interpolating polynomials p_N and $\tilde{p}_N$ for $N = 10$ on $[-1,1]$ using equispaced and CGL points respectively. From this figure it is seen that in case of equispaced the absolute error oscillates towards the end points (Runge phenomenon) while in case of CGL points the absolute error is not large.

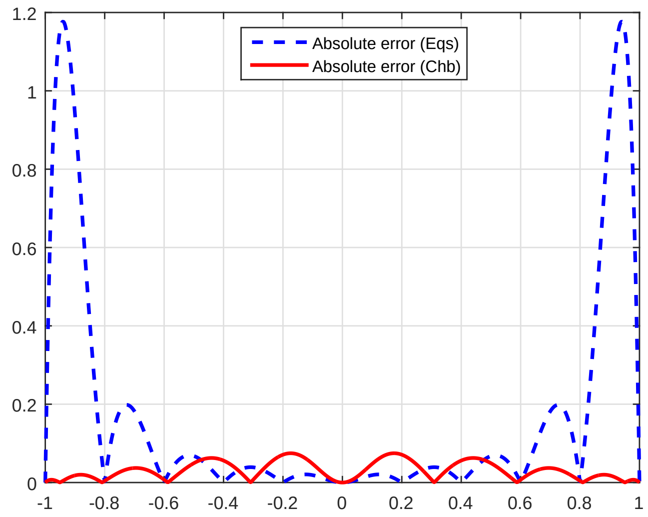

Figure 2.18: Graphs of the absolute error of f and its interpolating polynomials $p_N(x)$ and $\tilde{p}_N(x)$ for $N = 10$ on $[-1,1]$.

According to the application of CSCM, the following subsection is included to see how to obtain an approximation of the derivative f' from the Lagrange interpolation polynomial defined by (2.6).

2.2.3. Differentiation

In this subsection the differentiation of the interpolation polynomial is considered. Supposing that the polynomial p'_N which is an approximation to f' from the Lagrange interpolation polynomial defined by the relation (2.6) is to be obtained. The polynomial p'_N has the degree at most $N-1$ and is given as follows

$$p'_N(x) = \sum_{k=0}^{N} C'_k(x) f(x_k), \quad (N \geq 1). \tag{2.86}$$

The following theorem gives an expression for the difference between $f'(x)$ and the approximation $p'_N(x)$ which is proved in [10].

Theorem 2.8. Assume that $f \in C^{N+1}[a,b]$, and $x_0, x_1, \ldots, x_N$ are distinct interpolation points, and $p_N \in \mathscr{P}_N$ is the Lagrange interpolation polynomial for f. Then, there exist distinct points $\kappa_0, \kappa_1, \ldots, \kappa_N$ in (a,b), and corresponding to each x in $[a,b]$, there is

$\zeta = \zeta(x)$ *in* (a,b) *such that:*

$$f'(x) - p'_N(x) = \frac{f^{(N+1)}(\zeta)}{N!}\omega^\star_N(x), \text{ where } \omega^\star_N(x) = (x-\kappa_1)(x-\kappa_2)\cdots(x-\kappa_N). \tag{2.87}$$

The following corollary is included to illustrate the bound of error for the difference between f' and p'_N .

Corollary 2.2. Let $N \geq 1$, *and assume that* $f \in C^{N+1}[a,b]$. *Suppose that* $x_0, x_1, \ldots, x_N$ *are distinct interpolation points in the interval* $[a,b]$, *and* $p_N \in \mathscr{P}_N$ *the Lagrange interpolation polynomials for* f.

$$|f'(x) - p'_N(x)| \leq \frac{\Gamma_{N+1}}{N!}|\omega^\star_N(x)| \leq \frac{(b-a)^N \Gamma_{N+1}}{N!}, \quad \Gamma_{N+1} = \max_{a \leq x \leq b} |f^{(N+1)}(x)|. \tag{2.88}$$

Remark 2.1. If f *and all its derivatives are defined and continuous on* $[a,b]$, *and* $\lim_{N\to\infty} \frac{(b-a)^N \Gamma_{N+1}}{N!} = 0$, *then* $\lim_{N\to\infty} \max_{a\leq x\leq b} |f'(x) - p'_N(x)| = 0$. *This shows the uniform convergence on* $[a,b]$ *of the sequence of interpolation polynomial* p'_N *to* f'.

The following example is included to illustrate how the Corollary 2.2 can be used.

Example 2.7. Consider the function $f : x \mapsto e^x$ *on* $[-\alpha, \alpha]$, *where* $\alpha > 0$. *Assume that* f *is given at the* $x_0 = -\alpha$ *and* $x_1 = \alpha$, *and that* $f(-\alpha)$, $f(\alpha)$ *are known, however, up to given rounding errors* ε_- *and* ε_+ *respectively. Also assume that* $p_1 \in \mathscr{P}_1$ *is the Lagrange interpolation polynomial for* f *at* x_0 *and* x_1 *which is given as*

$$p_1(x) = \frac{e^\alpha - e^{-\alpha}}{2\alpha}(x+\alpha) + e^{-\alpha}. \tag{2.89}$$

Differentiating (2.89) with respect to x. It is obtained as $p'_1(x) \approx \frac{e^\alpha - e^{-\alpha}}{2\alpha}$. *Therefore,* $p'_1 \in \mathscr{P}_0$ *which represents an approximation to* $f'(0) = 1$ *at any* x *in the interval* $[-\alpha, \alpha]$. *However, only* $e^{-\alpha} + \varepsilon_-$ *and* $e^\alpha + \varepsilon_+$ *are available due to the presence of rounding errors, with unknown* ε_- *and* ε_+. *Therefore, it can be only calculated*

$$\frac{(e^\alpha + \varepsilon_+) - (e^{-\alpha} + \varepsilon_-)}{2\alpha}. \tag{2.90}$$

Equation (2.90) can be written as follows: $\frac{e^{\alpha}-e^{-\alpha}}{2\alpha}+\frac{\varepsilon_{+}-\varepsilon_{-}}{2\alpha}$*. Then,*

$$\lim_{\alpha\to 0}\left(\frac{e^{\alpha}-e^{-\alpha}}{2\alpha}-f'(0)\right)=0. \tag{2.91}$$

From (2.91), it is obtained that $\frac{e^{\alpha}-e^{-\alpha}}{2\alpha}$ *converges to* $f'(0)$ *as* α *tends to* 0*, while for* ε_{-} *and* ε_{+} *nonzero and fixed, the following applies,*

$$\lim_{\alpha\to 0}\left(\frac{\varepsilon_{+}-\varepsilon_{-}}{2\alpha}\right)=\infty. \tag{2.92}$$

Remark 2.2. The approximation of $f'(0)$ *might not be accurate due to a large error whose size is* $\frac{|\varepsilon_{+}-\varepsilon_{-}|}{2\alpha}$ *when* α *becomes too small in comparison with* $|\varepsilon_{+}-\varepsilon_{-}|$*, while* $\frac{|\varepsilon_{+}-\varepsilon_{-}|}{2\alpha}$ *might be small when* α *becomes very large in comparison with* $|\varepsilon_{+}-\varepsilon_{-}|$*. Therefore, the existence of an optimal* α *that depends on the magnitude of the rounding error is shown by these observations, where the error between* $f'(0)$ *and the approximation (2.90) is smallest.*

Consider $E(\alpha)=\frac{(e^{\alpha}+\varepsilon_{+})-(e^{-\alpha}+\varepsilon_{-})}{2\alpha}-f'(0)$.
By expanding $e^{-\alpha}$ and e^{α} into Taylor series about point $x=0$, it is obtained as:

$$e^{-\alpha}=f(0)-\alpha f'(0)+\frac{1}{2}\alpha^{2}f''(0)-\frac{1}{6}\alpha^{3}f'''(\zeta_{1}), \tag{2.93}$$

and

$$e^{\alpha}=f(0)+\alpha f'(0)+\frac{1}{2}\alpha^{2}f''(0)+\frac{1}{6}\alpha^{3}f'''(\zeta_{2}), \tag{2.94}$$

where $\zeta_{1}\in(-\alpha,0)$ and $\zeta_{2}\in(0,\alpha)$.
Subtracting equation (2.94) from (2.93), it is obtained as

$$e^{\alpha}-e^{-\alpha}=2\alpha f'(0)+\frac{1}{6}\alpha^{3}(f'''(\zeta_{1})+f'''(\zeta_{2})). \tag{2.95}$$

The fact that there exists $f'''(x)=e^{x}$ which is continuous at all $x\in[-\alpha,\alpha]$, this implies the existence of ζ in $(-\alpha,\alpha)$ such that $f'''(\zeta)=\frac{1}{2}(f'''(\zeta_1)+f'''(\zeta_2))$. Moreover, by using (2.95) it is obtained as

$$\frac{e^{\alpha}-e^{-\alpha}}{2\alpha}-f'(0)=\frac{1}{6}\alpha^2 f'''(\zeta), \tag{2.96}$$

and hence

$$E(\alpha)=\frac{1}{6}\alpha^2 f'''(\zeta)+\frac{\varepsilon_+-\varepsilon_-}{2\alpha}. \tag{2.97}$$

By taking the absolute value of both sides in the relation (2.97), the following applies

$$|E(\alpha)|=\left|\frac{1}{6}\alpha^2 f'''(\zeta)+\frac{\varepsilon_+-\varepsilon_-}{2\alpha}\right|\le\left|\frac{1}{6}\alpha^2 f'''(\zeta)\right|+\left|\frac{\varepsilon_+-\varepsilon_-}{2\alpha}\right|. \tag{2.98}$$

By bounding $|f'''(\zeta)|$ by $\Gamma_3=\max\limits_{x\in[-\alpha,\alpha]}|f'''(x)|$, and then $|\varepsilon_+|$ and $|\varepsilon_-|$ by ε, then the result

$$|E(\alpha)|\le\frac{1}{6}\alpha^2\Gamma_3+\frac{\varepsilon}{\alpha}. \tag{2.99}$$

Let $K(\alpha)$ be the right-hand side of the relation (2.99) as a function of $\alpha>0$, this function is positive. We need to have the value of α for which the bound on $|E(\alpha)|$ is minimized. Setting the derivative of $K(\alpha)=\frac{1}{6}\alpha^2\Gamma_3+\frac{\varepsilon}{\alpha}$ to 0, the following applies

$$\frac{1}{3}\alpha\Gamma_3-\frac{\varepsilon}{\alpha^2}=0, \tag{2.100}$$

and hence,

$$\alpha=\left(\frac{3\varepsilon}{\Gamma_3}\right)^{\frac{1}{3}}, \tag{2.101}$$

which gives the value of α for which the bound on $|E(\alpha)|$ is minimized.

Table 2.8: Values of $p_1'(x)$ and $|E(\alpha)|$ with different values of α.

α	$p_1'(x)$	$\lvert E(\alpha)\rvert$
0.1	1.0017	0.0017
0.01	1.000	0
$\vdots$	$\vdots$	$\vdots$
10^{-12}	1.000	0
10^{-13}	0.9998	0.0002
10^{-14}	0.9992	0.0008
10^{-15}	1.0547	0.0547
10^{-16}	0.5551	0.4449
10^{-17}	0	1

Table 2.8 shows $p_1'(x)$ which represents an approximation to $f'(0) = 1$, and $|E(\alpha)|$ the error between $f'(0)$ and the approximation (2.90) for several values of α. From Table 2.8, it can be seen that for $\alpha = 0.01$ up to 10^{-12}, $p_1'(x)$ approximates well $f'(0)$ which is equal to 1, while for $\alpha = 0.1$, $p_1'(x) = 1.0017$ and for $\alpha = 10^{-15}$, $p_1'(x) = 1.0547$. Furthermore, for $\alpha = 10^{-13}$ and $\alpha = 10^{-16}$, $p_1'(x) = 0.9998$ and $p_1'(x) = 0.5551$ respectively, and then for $\alpha = 10^{-17}$, $p_1'(x) = 0$.

The graphs and tables of the maximum error in the infinity norm of the difference between f and; each of p_N and $\tilde{p}_N$ with equispaced ($\|f - p_N\|_\infty$) and CGL points ($\|f - \tilde{p}_N\|_\infty$), and, f' and; each of p_N' and $\tilde{p}_N'$ with equispaced ($\|f' - p_N'\|_\infty$) and CGL points ($\|f' - \tilde{p}_N'\|_\infty$), are given in that follows.

For that, the first case $f_1(x) = e^x \sin(5x)$, and the second case $f_2(x) = \sin(10x)$ are considered. It is known that $f_1'(x) = e^x(\sin(5x) + 5\cos(5x))$, and $f_2'(x) = 10\cos(10x)$.

Table 2.9: Comparison of $\|f_1 - p_N\|_\infty$, $\|f_1 - \tilde{p}_N\|_\infty$ and $\|f_1' - p_N'\|_\infty$, $\|f_1' - \tilde{p}_N'\|_\infty$.

N	$\|f_1 - p_N\|_\infty$	$\|f_1 - \tilde{p}_N\|_\infty$	$\|f_1' - p_N'\|_\infty$	$\|f_1' - \tilde{p}_N'\|_\infty$
5	6.7499×10^{-1}	5.3279×10^{-1}	7.9959	4.6414
10	5.8674×10^{-3}	8.7306×10^{-4}	3.7807	0.0225
20	2.1520×10^{-9}	1.3768×10^{-11}	1.8336	6.7161×10^{-10}
50	5.9108×10^{-4}	3.1086×10^{-15}	0.7274	4.9094×10^{-13}

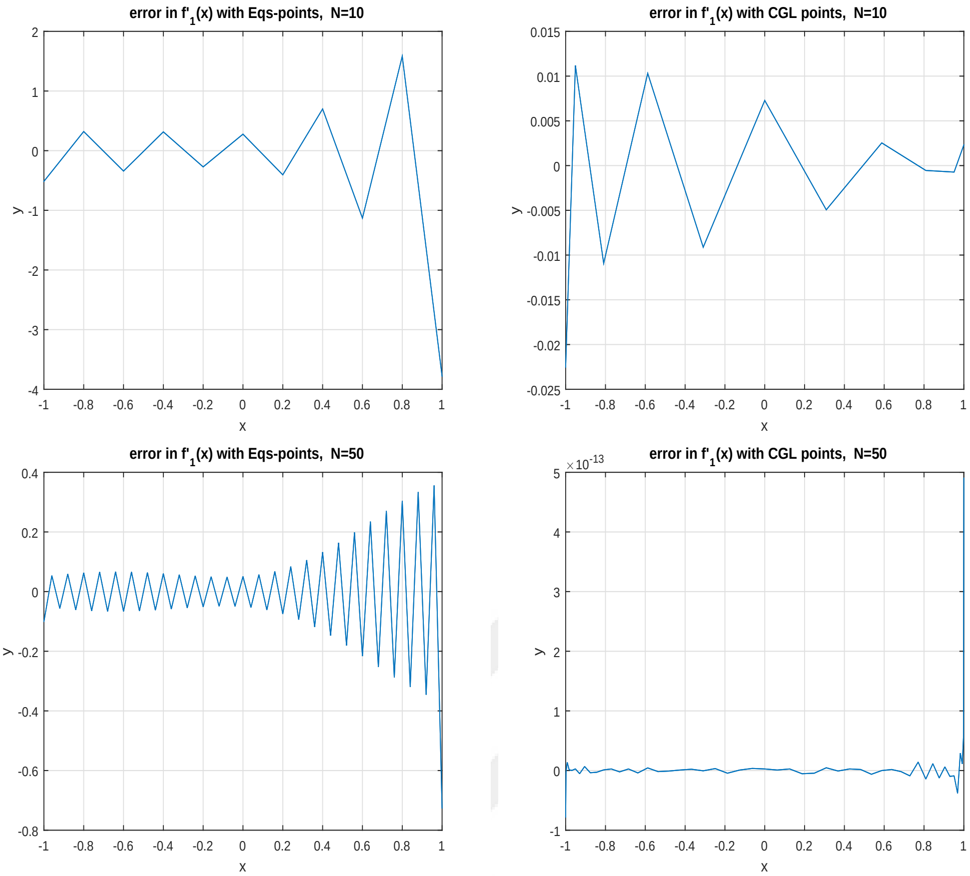

Figure 2.19: Graphs of $\|f_1' - p_N'\|_\infty$ (left) and $\|f_1' - \tilde{p}_N'\|_\infty$ (right) on $[-1, 1]$.

Table 2.9 presents the maximum error in the infinity norm of the difference between f_1 and; each of p_N, and $\tilde{p}_N$ for x in the interval $[-1, 1]$ using equispaced and CGL points respectively, for several values of N from 5 up to 50. From this table it is observed that the maximum error in the infinity norm of the difference between f_1 and p_N decreases when N increases. Furthermore, it can be seen that the maximum error in the infinity norm of the difference between f_1 and $\tilde{p}_N$ decreases when N increases. When compared with the results obtained by using equispaced points, it is observed that the results obtained by using CGL points give more accurate approximations than obtained by equispaced points. In the same way, in the case of differentiation, the results obtained by using CGL points give more accurate approximations those obtained by equispaced points.

Figure 2.19 shows the graphs of $\|f_1' - p_N'\|_\infty$ and $\|f_1' - \tilde{p}_N'\|_\infty$ for $N = 10$ and $N = 50$ on $[-1, 1]$ using equispaced points and CGL points respectively. It is observed that the maximum error in the infinity norm of the difference between f_1' and p_N', and, f_1' and $\tilde{p}_N'$ decreases as N increases. Moreover, It is also seen that for the case using

CGL points for $N = 50$, the results give a good approximation.

Table 2.10: Comparison of $\|f_2 - p_N\|_\infty$, $\|f_2 - \tilde{p}_N\|_\infty$ and $\|f_2' - p_N'\|_\infty$, $\|f_2' - \tilde{p}_N'\|_\infty$.

N	$\|f_2 - p_N\|_\infty$	$\|f_2 - \tilde{p}_N\|_\infty$	$\|f_2' - p_N'\|_\infty$	$\|f_2' - \tilde{p}_N'\|_\infty$
5	2.7141	1.4238	13.9000	11.3219
10	2.4663	6.0413×10^{-1}	2.7645	6.2859
20	1.7445×10^{-3}	1.2239×10^{-5}	1.2076	3.9430×10^{-4}
50	9.7587×10^{-4}	2.1094×10^{-15}	0.4682	4.3165×10^{-13}

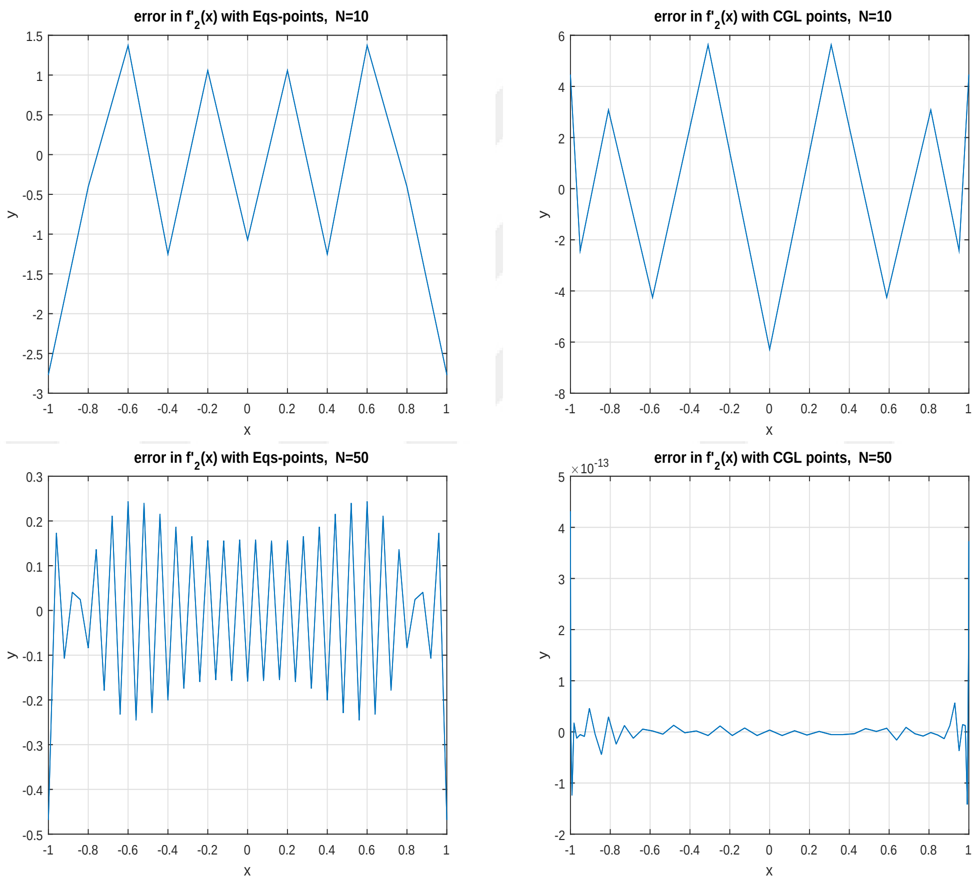

Figure 2.20: Graphs of $\|f_2' - p_N'\|_\infty$ (left) and $\|f_2' - \tilde{p}_N'\|_\infty$ (right) on $[-1, 1]$.

Table 2.10 presents the maximum error in the infinity norm of the difference between f_2 and; each of p_N, and $\tilde{p}_N$ for x in the interval $[-1, 1]$ using equispaced and CGL points respectively, for several values of N from 5 up to 50. From this table it is observed that the maximum error in the infinity norm of the difference between f_2 and p_N decreases when N increases. Further, it can be seen that the maximum error in the infinity norm of the difference between f_2 and $\tilde{p}_N$ decreases when N increases.

When compared to the results obtained by using equispaced points, it is observed that the results obtained by using CGL points give a more accurate approximations than those obtained by equispaced points. In the same way, it can be seen that in the case of differentiation, the results obtained by using CGL points give more accurate approximations than those obtained by equispaced points.

Figure 2.20 shows the graphs of $\|f_2' - p_N'\|_\infty$ and $\|f_2' - \tilde{p}_N'\|_\infty$ for $N = 10$ and $N = 50$ on $[-1,1]$ using equispaced points and CGL points respectively. It can be seen that the maximum error in the infinity norm of the difference between f_2' and p_N', and, f_2' and $\tilde{p}_N'$ decreases as N increases. Furthermore, it is observed that there is a good approximation for the case using CGL points than that of the case using equispaced for $N = 50$.

As a conclusion, in this chapter, the theory of polynomial interpolation has been included with the existence and uniqueness of Lagrange interpolation polynomial. In estimating the error that exists between the function and its interpolating polynomial, it is shown generally that, the convergence that is expected to occur does not happen, and for this reason it is necessary that the error is carefully evaluated. The Runge phenomenon is discussed and then, the solution to the problem arising from this phenomenon is considered by placing special points. Moreover, polynomial approximation in the infinity norm is used to determine differences in the function and its interpolating polynomial. Because of this, the best approximation of degree N is stated and examples are provided. After this, the Lebesgue function and the Lebesgue constant are evaluated. The Lebesgue constant gives an idea on the closeness of Lagrange polynomial to the best approximation polynomial of degree N. Three sets of points, namely, the equispaced points, the CG points and the CGL points are used. It is observed that, among these sets of points, the CGL option is the most accurate. Finally, differentiation is also stated and with examples given.

3. NUMERICAL SOLUTIONS OF MHD EQUATIONS USING CHEBYSHEV SPECTRAL COLLOCATION METHOD

In this chapter, the numerical solutions of MHD flow equations using CSCM are presented. The CSCM relies on the interpolating polynomials which are defined on a set of CGL points where the differential equations are discretized to approximate the unknown functions. The polynomials are analytically differentiated, and for derivative approximation a differentiation matrix is constructed. The derivatives of higher order can easily be obtained by the multiplication of lower order matrices if a careful technique is considered to reduce the rounding errors induced. This makes the procedure computationally simple and achieves a high order accuracy for small sized problems. Thus, the method is used extensively in simple geometries. The main goal of this chapter is to use the convenience of CSCM with high order accuracy to approximate MHD equations. Section 3.1 describes the method of obtaining the differentiation matrices and the details of the collocation approach using CGL points. Applications of CSCM to $2D$ incompressible, MHD problems are presented in Section 3.2. The CSCM solutions to one-dimensional MHD Couette flow are presented in Section 3.3.1. Additionally, the application of CSCM to the two-dimensional forced MHD flow problem with analytical solution is presented in Section 3.3.2. In Section 3.3.3, the application of CSCM to the two-dimensional fluid flow problems, laminar, transient, incompressible MHD flow subjected to an externally applied magnetic field, with attention to the induced magnetic field in a regularized lid-driven cavity is considered.

3.1. Chebyshev Spectral Collocation Method

The basic idea in CSCM is to require the numerical approximation p_N of a solution f to a boundary value problem

$$\begin{aligned} \mathfrak{D} f &= g \\ \mathfrak{B} f &= h \end{aligned} \tag{3.1}$$

to be exactly satisfied on a set of predefined points called the collocation points. In (3.1) $\mathfrak{B}$ is the boundary operator, $\mathfrak{D}$ is the differential operator, h and g are respectively known functions in the problem domain and on the boundary. In this method, the solution f is generally interpolated at the collocation points which are taken as CGL points defined in the previous chapter. Moreover, the derivatives of f are approximated by the derivatives of p_N. Due to the desired property of uneven distribution in the standard interval, the CGL points are widely used in interpolation, where most of them are gathered near the endpoints on the interval.

Recall that in the previous chapter the Chebyshev polynomial of the first kind $T_N(x)$ of degree N on the interval $[-1,1]$ and the recurrence relation were defined. The recurrence relation on the derivative is given as

$$\frac{T'_{N+1}(x)}{2(N+1)} - \frac{T'_{N-1}(x)}{2(N-1)} = T_N(x), \quad \text{for } N > 1. \tag{3.2}$$

Previously, it is seen that $f \in C[-1,1]$ can be approximated by p_N of degree at most N of the form [23]-[15]

$$p_N(x) = \sum_{j=0}^{N} C_j(x) f(x_j^{CGL}), \tag{3.3}$$

with $p_N(x_j^{CGL}) = f(x_j^{CGL})$, and $C_j(x)$ is a Lagrange basis function of degree N defined as [24]

$$\begin{aligned} C_j(x) &= (-1)^{i+j} \frac{(1-x^2)T'_N(x)}{\gamma_j N^2 (x - x_j^{CGL})} \quad \text{for } j = 0,1,\ldots,N \\ &= \frac{2}{N\varsigma_j} \sum_{l=0}^{N} \frac{1}{\varsigma_l} T_l(x_j^{CGL}) T_l(x). \end{aligned} \tag{3.4}$$

In the previous chapter the CGL points on $[-1,1]$ are given as $x_j^{CGL} = \cos\left(\frac{j\pi}{N}\right)$, and $\gamma_0 = \gamma_N = 2$, and $\gamma_j = 1$ for $j = 1,...,N-1$.

$$C_j(x_k) = \delta_{jk} \quad \text{for } j,k = 0,1,\ldots,N \tag{3.5}$$

and $\varsigma_j = 2$ for $j = 0, N$, $\varsigma_j = 1$ if $j = 1,\ldots,N-1$. The derivatives of the approximate solution p_N are estimated by derivation of (3.4) at the collocation points and evaluated by expression (3.3). This gives

$$p_N^{(m)}(x) = \sum_{j=0}^{N} C_j^{(m)}(x) f(x_j^{CGL}). \tag{3.6}$$

At the CGL points, the first derivative satisfies $C_j^{(1)}(x_i) = d_{ij}$ where

$$\begin{aligned} d_{00} &= \frac{2N^2+1}{6}, \\ d_{NN} &= -d_{00}, \\ d_{ij} &= \frac{\varsigma_i(-1)^{i+j}}{\varsigma_j(x_i - x_j^{CGL})} \quad j \neq i, \quad j,i = 1,\ldots,N-1. \end{aligned} \tag{3.7}$$

In order to obtain the discrete values of the first derivative of f the following applies

$$p_N^{(1)}(x) = \sum_{j=0}^{N} d_{ij} f(x_j^{CGL}). \tag{3.8}$$

In matrix-vector form, Equation (3.8) can be written as

$$\frac{d}{dx}\{p_N\} = [D_N^{(1)}]\{p_N\}, \tag{3.9}$$

where $\{p_N\} = \left[p_N(x_0^{CGL}), p_N(x_1^{CGL}), \ldots, p_N(x_N^{CGL})\right]^T$, and $[D_N^{(1)}] = [d_{ij}]$ is the first order Chebyshev differentiation matrix (CDM) which is of size $(N+1) \times (N+1)$, [23]-[15].

In order to calculate the first derivatives, the round off errors are minimized by computing the diagonal entries d_{ii} as [15]

$$d_{ii} = -\sum_{\substack{j=0 \\ j\neq i}}^{N} d_{ij}. \tag{3.10}$$

The m-th order derivative of the function $f(x)$ is approximated by

$$\frac{d^m}{dx^m}\{p_N\} = [D_N^{(m)}]\{p_N\}, \tag{3.11}$$

where $[D_N^{(m)}] = [D_N^{(1)}]^m$ and m denotes the usual matrix multiplication m-times. $[D_N^{(m)}]$ is referred as the m-th order CDM. The CGL points on an arbitrary interval $[a,b]$ can be taken by a linear transformation as

$$x_j^{CGL} = \frac{b-a}{2}\cos\left(\frac{j\pi}{N}\right) + \frac{a+b}{2}, \quad \text{where } j = 0,1,\ldots,N. \tag{3.12}$$

A sample distribution of the CGL points used as collocation points on a 16×16 grid in the problem domain is illustrated in Figure 3.1, where it can be seen that the collocation points gather through the boundaries.

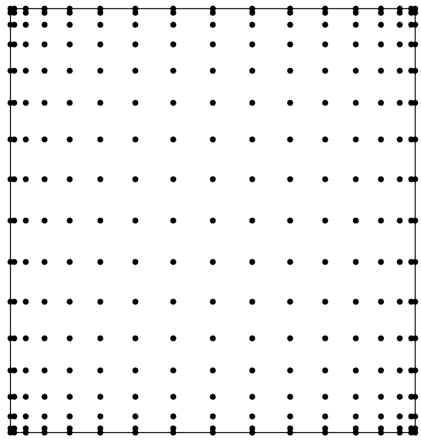

Figure 3.1: A sample CGL points distribution of a square region using $N = 16$.

3.2. Applications Of CSCM To MHD Equations

This section presents the applications of the Chebyshev spectral collocation method to $2D$ incompressible, steady, MHD flow problems. As mentioned in Chapter 1, the MHD equations are obtained by coupling the Maxwell's equations with N-S equations by means of Ohm's law. The governing equations can be formulated in terms of u and v the respective x-and y-components of the velocity of the fluid, pressure p, intensity of the magnetic field B_x and B_y.

The non-dimensional governing equations for incompressible MHD flow problems are given as [8]

$$\frac{\partial u}{\partial x}+\frac{\partial v}{\partial y}=0, \tag{3.13}$$

$$u\frac{\partial u}{\partial x}+v\frac{\partial u}{\partial y}=-\frac{\partial p}{\partial x}+\frac{1}{Re}\left(\frac{\partial^2 u}{\partial x^2}+\frac{\partial^2 u}{\partial y^2}\right)-\frac{Ha^2}{Re_m Re}B_y\left(\frac{\partial B_y}{\partial x}-\frac{\partial B_x}{\partial y}\right) \tag{3.14a}$$

$$u\frac{\partial v}{\partial x}+v\frac{\partial v}{\partial y}=-\frac{\partial p}{\partial y}+\frac{1}{Re}\left(\frac{\partial^2 v}{\partial x^2}+\frac{\partial^2 v}{\partial y^2}\right)+\frac{Ha^2}{Re_m Re}B_x\left(\frac{\partial B_y}{\partial x}-\frac{\partial B_x}{\partial y}\right), \tag{3.14b}$$

$$\frac{\partial B_x}{\partial x}+\frac{\partial B_y}{\partial y}=0, \tag{3.15}$$

$$\frac{1}{Re_m}\left(\frac{\partial^2 B_x}{\partial x^2}+\frac{\partial^2 B_x}{\partial y^2}\right)+\frac{\partial}{\partial y}(uB_y-vB_x)=0, \tag{3.16a}$$

$$\frac{1}{Re_m}\left(\frac{\partial^2 B_y}{\partial x^2}+\frac{\partial^2 B_y}{\partial y^2}\right)-\frac{\partial}{\partial x}(uB_y-vB_x)=0, \tag{3.16b}$$

where Re, Re_m, and Ha represent respectively, the Reynolds number, the magnetic Reynolds number, and the Hartmann number. Equations in (3.13) and (3.14) are obtained from the N-S equations namely the continuity and momentum equations, respectively, whereas the equations (3.15) and (3.16) are obtained from Maxwell's equations. The divergence-free condition for the magnetic field given in (1.4) could be considered as redundant. The system can be numerically solved without using this equation. In order to reduce the Maxwell equations in the continuous level, the previous condition (1.4) is implied in combination of Ampere's and Ohm's laws as described in Chapter 1.

Equations in (3.13) and (3.14) accurately constitute the fluid flow phenomena, however, the pressure terms in the momentum equations cause difficulties in the direct solution of these equations. Consequently, many researchers have introduced alternative formulations to represent these equations. The formulation of the stream function-vorticity is one of these methodologies for the $2D$ flow. In order to obtain this formulation, stream function ψ satisfying the equation (3.13) automatically is given as

$$u=\frac{\partial \psi}{\partial y}, \qquad v=-\frac{\partial \psi}{\partial x}. \tag{3.17}$$

From (3.17), by substituting u and v in the equation (3.13), it is obtained that,

$$\frac{\partial u}{\partial x}+\frac{\partial v}{\partial y}=\frac{\partial^2\psi}{\partial x\partial y}-\frac{\partial^2\psi}{\partial x\partial y}=0. \tag{3.18}$$

Thus, the continuity equation is satisfied. The non-zero component of the vorticity field w in a $2D$ flow is defined as

$$w=\frac{\partial v}{\partial x}-\frac{\partial u}{\partial y}. \tag{3.19}$$

From (3.17), by substituting u and v in the equation (3.19), results in the following

$$\begin{aligned} w &= \frac{\partial v}{\partial x}-\frac{\partial u}{\partial y} \\ &= -\frac{\partial^2\psi}{\partial x^2}-\frac{\partial^2\psi}{\partial y^2} \\ &= -\nabla^2\psi \\ &= -\Delta\psi. \end{aligned} \tag{3.20}$$

Therefore, the relation between w and ψ is given by $w=-\Delta\psi$.

In analogy to the stream function vorticity formulation, a natural approach is to introduce the magnetic stream function A relating to the magnetic field components as follows

$$B_x=\frac{\partial A}{\partial y}, \quad B_y=-\frac{\partial A}{\partial x}. \tag{3.21}$$

The current density J is defined as

$$J=\frac{\partial B_y}{\partial x}-\frac{\partial B_x}{\partial y}. \tag{3.22}$$

Now, it is possible to eliminate the pressure terms in the equations (3.14) by subtracting the derivative of the first equation of (3.14) with respect to y, from the derivative of the second equation of (3.14) with respect to x. This is done to avoid handling the pressure as it has no physical boundary conditions.

Let H_L be the left hand side of the resulting equation, and H_R the right hand side. Then, H_L gives

$$
\begin{aligned}
H_L &= \frac{\partial}{\partial x}\left(u\frac{\partial v}{\partial x}+v\frac{\partial v}{\partial y}\right)-\frac{\partial}{\partial y}\left(u\frac{\partial u}{\partial x}+v\frac{\partial u}{\partial y}\right)\\
&= \frac{\partial u}{\partial x}\frac{\partial v}{\partial x}+u\frac{\partial v}{\partial x^2}+\frac{\partial v}{\partial x}\frac{\partial v}{\partial y}+v\frac{\partial^2 v}{\partial x\partial y}\\
&\quad -\frac{\partial u}{\partial y}\frac{\partial u}{\partial x}-u\frac{\partial^2 u}{\partial x\partial y}-\frac{\partial v}{\partial y}\frac{\partial u}{\partial y}-v\frac{\partial u}{\partial y^2}\\
&= \frac{\partial v}{\partial x}\underbrace{\left(\frac{\partial u}{\partial x}+\frac{\partial v}{\partial y}\right)}_{=0}+u\frac{\partial v}{\partial x^2}+v\frac{\partial^2 v}{\partial x\partial y}\\
&\quad -\frac{\partial u}{\partial y}\underbrace{\left(\frac{\partial u}{\partial x}+\frac{\partial v}{\partial y}\right)}_{=0}-u\frac{\partial^2 u}{\partial x\partial y}-v\frac{\partial u}{\partial y^2}\\
&= u\frac{\partial v}{\partial x^2}+v\frac{\partial^2 v}{\partial x\partial y}-u\frac{\partial^2 u}{\partial x\partial y}-v\frac{\partial u}{\partial y^2}\\
&= u\underbrace{\left(\frac{\partial v}{\partial x}-\frac{\partial u}{\partial y}\right)_x}_{w_x}+v\underbrace{\left(\frac{\partial v}{\partial x}-\frac{\partial u}{\partial y}\right)_y}_{w_y}\\
&= uw_x+vw_y\\
&= u\frac{\partial w}{\partial x}+v\frac{\partial w}{\partial y}\\
H_L &= \frac{\partial \psi}{\partial y}\frac{\partial w}{\partial x}-\frac{\partial \psi}{\partial x}\frac{\partial w}{\partial y}.
\end{aligned}
\tag{3.23}
$$

And H_R gives,

$$
\begin{aligned}
H_R &= \frac{1}{Re}\left(\frac{\partial^3 v}{\partial x^3} - \frac{\partial^3 u}{\partial x^2 \partial y} + \frac{\partial^3 v}{\partial x \partial y^2} - \frac{\partial^3 u}{\partial y^3}\right) \\
&\quad + \frac{Ha^2}{Re_m Re}\left(\frac{\partial B_x}{\partial x}\frac{\partial B_y}{\partial x} - \frac{\partial B_x}{\partial y}\frac{\partial B_x}{\partial x} + B_x \frac{\partial B_y}{\partial x^2} - B_x \frac{\partial^2 B_y}{\partial x \partial y}\right) \\
&\quad + \frac{Ha^2}{Re_m Re}\left(\frac{\partial B_y}{\partial y}\frac{\partial B_y}{\partial x} - \frac{\partial B_y}{\partial y}\frac{\partial B_x}{\partial y} + B_y \frac{\partial^2 B_y}{\partial x \partial y} - B_y \frac{\partial B_x}{\partial y^2}\right) \\
&= \frac{1}{Re}\left\{\frac{\partial^2}{\partial x^2}\underbrace{\left(\frac{\partial v}{\partial x} - \frac{\partial u}{\partial y}\right)}_{w} + \frac{\partial^2}{\partial y^2}\underbrace{\left(\frac{\partial v}{\partial x} - \frac{\partial u}{\partial y}\right)}_{w}\right\} \\
&\quad + \frac{Ha^2}{Re_m Re}\left\{\frac{\partial B_x}{\partial x}\underbrace{\left(\frac{\partial B_y}{\partial x} - \frac{\partial B_x}{\partial y}\right)}_{J} + \frac{\partial B_y}{\partial y}\underbrace{\left(\frac{\partial B_y}{\partial x} - \frac{\partial B_x}{\partial y}\right)}_{J}\right\} \\
&\quad + \frac{Ha^2}{Re_m Re}\left\{B_y \underbrace{\left(\frac{\partial B_y}{\partial x} - \frac{\partial B_x}{\partial y}\right)_y}_{J_y} + B_x \underbrace{\left(\frac{\partial B_y}{\partial x} - \frac{\partial B_x}{\partial y}\right)_x}_{J_x}\right\} \\
&= \frac{1}{Re}\underbrace{(w_{xx} + w_{yy})}_{\Delta w} + \frac{Ha^2}{Re_m Re}\left\{\frac{\partial B_x}{\partial x}J + \frac{\partial B_y}{\partial y}J + B_x J_x + B_y J_y\right\} \\
&= \frac{1}{Re}\Delta w + \frac{Ha^2}{Re_m Re}\left\{J \underbrace{\left(\frac{\partial B_x}{\partial x} + \frac{\partial B_y}{\partial y}\right)}_{=0} + B_x J_x + B_y J_y\right\} \\
&= \frac{1}{Re}\Delta w + \frac{Ha^2}{Re_m Re} + (B_x J_x + B_y J_y) \\
H_R &= \frac{1}{Re}\Delta w + \frac{Ha^2}{Re_m Re} + \left(\frac{\partial A}{\partial y}\frac{\partial J}{\partial x} - \frac{\partial A}{\partial x}\frac{\partial J}{\partial y}\right).
\end{aligned}
\tag{3.24}
$$

Therefore, Equation (3.14) can be expressed in terms of ψ, w, A and J as follows:

$$
\frac{\partial \psi}{\partial y}\frac{\partial w}{\partial x} - \frac{\partial \psi}{\partial x}\frac{\partial w}{\partial y} = \frac{1}{Re}\Delta w + \frac{Ha^2}{Re_m Re} + \left(\frac{\partial A}{\partial y}\frac{\partial J}{\partial x} - \frac{\partial A}{\partial x}\frac{\partial J}{\partial y}\right). \tag{3.25}
$$

Thus, from Equation (3.25), the following applies:

$$
\Delta w = Re\left(\frac{\partial \psi}{\partial y}\frac{\partial w}{\partial x} - \frac{\partial \psi}{\partial x}\frac{\partial w}{\partial y}\right) - \frac{Ha^2}{Re_m}\left(\frac{\partial A}{\partial y}\frac{\partial J}{\partial x} - \frac{\partial A}{\partial x}\frac{\partial J}{\partial y}\right). \tag{3.26}
$$

Similar to the above deduction, Equations (3.15)-(3.16) can be obtained. The left hand side gives

$$
\begin{aligned}
\frac{1}{Re_m}\left\{\frac{\partial^3 B_y}{\partial x^3}-\frac{\partial^3 B_x}{\partial x^2 \partial y}+\frac{\partial^3 B_y}{\partial x \partial y^2}-\frac{\partial^3 B_x}{\partial y^3}\right\} &= \frac{1}{Re_m}\left\{\frac{\partial^2}{\partial x^2}\underbrace{\left(\frac{\partial B_y}{\partial x}-\frac{\partial B_x}{\partial y}\right)}_{J}\right\} \\
&+\frac{1}{Re_m}\left\{\frac{\partial^2}{\partial y^2}\underbrace{\left(\frac{\partial B_y}{\partial x}-\frac{\partial B_x}{\partial y}\right)}_{J}\right\} \\
&= \frac{1}{Re_m}\left(\frac{\partial^2 J}{\partial x^2}+\frac{\partial^2 J}{\partial y^2}\right).
\end{aligned} \tag{3.27}
$$

The right hand side gives

$$
\frac{\partial^2}{\partial x^2}(uB_y - vB_x) - \left\{-\frac{\partial^2}{\partial y^2}(uB_y - vB_x)\right\} = \left(\frac{\partial^2}{\partial x^2}+\frac{\partial^2}{\partial y^2}\right)(uB_y - vB_x). \tag{3.28}
$$

Hence, it is obtained as

$$
\frac{1}{Re_m}\left(\frac{\partial^2 J}{\partial x^2}+\frac{\partial^2 J}{\partial y^2}\right) = \left(\frac{\partial^2}{\partial x^2}+\frac{\partial^2}{\partial y^2}\right)(uB_y - vB_x). \tag{3.29}
$$

Thus, from the equation (3.29) the following is obtained

$$
\Delta J = Re_m \Delta(uB_y - vB_x). \tag{3.30}
$$

In non-dimensional form, Equation (3.22) can be expressed in terms of A and J as:

$$
\begin{aligned}
J &= \frac{\partial B_y}{\partial x}-\frac{\partial B_x}{\partial y} \\
&= -\frac{\partial^2 A}{\partial x^2}-\frac{\partial^2 A}{\partial y^2} \\
J &= -\Delta A.
\end{aligned} \tag{3.31}
$$

Hence, it is obtained as $\Delta A = -J$.

Consequently, the governing equations are nonlinear system of PDEs, coupled, and are given as [8]

$$\begin{aligned}
&\Delta\psi = -w,\\
&\Delta w = Re\left(\frac{\partial\psi}{\partial y}\frac{\partial w}{\partial x} - \frac{\partial\psi}{\partial x}\frac{\partial w}{\partial y}\right) - \frac{Ha^2}{Re_m}\left(\frac{\partial A}{\partial y}\frac{\partial J}{\partial x} - \frac{\partial A}{\partial x}\frac{\partial J}{\partial y}\right),\\
&\Delta A = -J,\\
&\Delta J = Re_m\Delta(uB_y - vB_x).
\end{aligned} \tag{3.32}$$

In the equations above, the dimensionless parameters Re, Ha and Re_m are given as described in Chapter 1. The equations defined in (3.32) are nonlinear, then to solve these equations, an iterative procedure to approximate the solution of these equations is applied. For this reason, an artificial time, t, dependence is introduced into the problem. Thus, the equations to solve are given as follows:

$$\begin{aligned}
&\Delta\psi = -w,\\
&\frac{\partial w}{\partial t} = \Delta w - Re\left(\frac{\partial\psi}{\partial y}\frac{\partial w}{\partial x} - \frac{\partial\psi}{\partial x}\frac{\partial w}{\partial y}\right) + \frac{Ha^2}{Re_m}\left(\frac{\partial A}{\partial y}\frac{\partial J}{\partial x} - \frac{\partial A}{\partial x}\frac{\partial J}{\partial y}\right),\\
&\Delta A = -J,\\
&\frac{\partial J}{\partial t} = \Delta J + Re_m\Delta\left(\frac{\partial\psi}{\partial y}\frac{\partial A}{\partial x} - \frac{\partial\psi}{\partial x}\frac{\partial A}{\partial y}\right).
\end{aligned} \tag{3.33}$$

Now, the CSCM discretization is obtained by following the steps of Section 3.1 the first order CDM in the x-direction, as denoted by $[D_N^{(1)}] = [d_{ij}^{(1)}]$ is computed. The second order CDM in this direction is obtained by calculating the square of $D_N^{(1)}$ as follows $[D_N^{(2)}] = [d_{ij}^{(2)}]$, and in the same way differentiation matrices in the y-direction, $[E_N^{(1)}] = [e_{ij}^{(1)}]$ and $[E_N^{(2)}] = [e_{ij}^{(2)}]$ are computed. The unconditionally stable backward difference scheme

$$\left.\frac{\partial u}{\partial t}\right|^{m+1} = \frac{u^{(m+1)} - u^{(m)}}{\delta t} \tag{3.34}$$

is used for advancing in time direction. Having constructed the differentiation matrices, the approximations ψ_N to stream function, w_N to vorticity, A_N to magnetic stream function and J to current density are substituted into the equations (3.33) as:

$$d_{ij}^{(2)}(\psi_N)_{ij} + e_{ij}^{(2)}(\psi_N)_{ij} = -(w_N)_{ij}, \tag{3.35}$$

$$\frac{w_N^{(m+1)} - w_N^{(m)}}{\delta t} = d_{ij}^{(2)}(w_N)_{ij} + e_{ij}^{(2)}(w_N)_{ij} - ReG_{ij} - f_{ij}, \tag{3.36}$$

$$d_{ij}^{(2)}(A_N)_{ij} + e_{ij}^{(2)}(A_N)_{ij} = -(J_N)_{ij}, \tag{3.37}$$

$$\frac{J_N^{(m+1)} - J_N^{(m)}}{\delta t} = d_{ij}^{(2)}(J_N)_{ij} + e_{ij}^{(2)}(J_N)_{ij} + Re_m(d_{ij}^{(2)} + e_{ij}^{(2)})S_{ij}, \tag{3.38}$$

where $i, j = 0, 1, \ldots, N$, and $d_{ij}^{(N)}$ and $e_{ij}^{(N)}$ are Chebyshev spectral N-th derivative coefficients in x- and y- directions, respectively. Further,

$$f_{ij} = \frac{Ha^2}{Re_m}\left[e_{ij}^{(1)}(A_N)_{ij}d_{ij}^{(1)}(J_N)_{ij} - d_{ij}^{(1)}(A_N)_{ij}e_{ij}^{(1)}(J_N)_{ij}\right], \tag{3.39}$$

and,

$$G_{ij} = \left[e_{ij}^{(1)}(\psi_N)_{ij}d_{ij}^{(1)}(w_N)_{ij} - d_{ij}^{(1)}(\psi_N)_{ij}e_{ij}^{(1)}(w_N)_{ij}\right], \tag{3.40}$$

and

$$S_{ij} = \left[e_{ij}^{(1)}(\psi_N)_{ij}d_{ij}^{(1)}(A_N)_{ij} - d_{ij}^{(1)}(\psi_N)_{ij}e_{ij}^{(1)}(A_N)_{ij}\right]. \tag{3.41}$$

By using the Kronecker product $\otimes$, the discretized equations in (3.35)-(3.38) can be written in matrix-vector form.

For instance, $$\begin{pmatrix} \alpha & \beta \\ \theta & \gamma \end{pmatrix} \otimes \begin{pmatrix} a & b \\ c & d \end{pmatrix} = \left(\begin{array}{cc|cc} \alpha a & \alpha b & \beta a & \beta b \\ \alpha c & \alpha d & \beta c & \beta d \\ \hline \theta a & \theta b & \gamma a & \gamma b \\ \theta c & \theta d & \gamma c & \gamma d \end{array}\right).$$

Moreover, equations in (3.35) and (3.37) are written in matrix-vector notation as given in Section 3.2 as

$$K\psi_N^{(m+1)} = -w_N^{(m)}, \tag{3.42}$$

and

$$KA_N^{(m+1)} = -J_N^{(m)}. \tag{3.43}$$

Equations in (3.36) and (3.38) are written in matrix-vector notation respectively as follows

$$\begin{aligned}
\frac{w_N^{(m+1)} - w_N^{(m)}}{\delta t} &= Kw_N^{(m+1)} - Re\left\{\mathscr{F}(\psi^{(m+1)}, w_N^{(m+1)})\right\} \\
&\quad + \frac{Ha^2}{Re_m}\left\{\mathscr{F}(A_N^{(m+1)}, J_N^{(m+1)})\right\}, \\
w_N^{(m+1)} - w_N^{(m)} &= K\delta t w_N^{(m+1)} - \delta t Re\left\{\mathscr{F}(\psi^{(m+1)}, w_N^{(m+1)})\right\} \\
&\quad + \frac{Ha^2}{Re_m}\delta t\left\{\mathscr{F}(A_N^{(m+1)}, J_N^{(m+1)})\right\}, \\
\left[I - K\delta t + \delta t Re\left\{\mathscr{F}(\psi^{(m+1)}, \iota)\right\}\right] w_N^{(m+1)} &= w_N^{(m)} \\
&\quad + \frac{Ha^2}{Re_m}\delta t\left\{\mathscr{F}(A_N^{(m+1)}, J_N^{(m+1)})\right\}, \\
\left[I - \delta t\left(Re\left\{\mathscr{F}(\psi^{(m+1)}, \iota)\right\} - K\right)\right] w_N^{(m+1)} &= w_N^{(m)} \\
&\quad + \frac{Ha^2}{Re_m}\delta t\left\{\mathscr{F}(A_N^{(m+1)}, J_N^{(m+1)})\right\}.
\end{aligned} \tag{3.44}$$

Hence, equations in (3.36) is expressed in matrix-vector notation as $\left[I - \delta t\left(Re\left\{\mathscr{F}(\psi^{(m+1)}, \iota)\right\} - K\right)\right] w_N^{(m+1)} = w_N^{(m)} + \frac{Ha^2}{Re_m}\delta t\left\{\mathscr{F}(A_N^{(m+1)}, J_N^{(m+1)})\right\}$, and for the equation in (3.38) the following applies

$$\begin{aligned}
\frac{J_N^{(m+1)} - J_N^{(m)}}{\delta t} &= KJ_N^{(m+1)} + Re_m\mathscr{F}(\psi^{(m+1)}, A_N^{(m+1)}), \\
J_N^{(m+1)} - J_N^{(m)} &= K\delta t J_N^{(m+1)} + Re_m\delta t\mathscr{F}(\psi^{(m+1)}, A_N^{(m+1)}), \\
[I - K\delta t]J_N^{(m+1)} &= J_N^{(m)} + Re_m\delta t\mathscr{F}(\psi^{(m+1)}, A_N^{(m+1)}).
\end{aligned} \tag{3.45}$$

Hence, equations in (3.33) is written in matrix-vector notation as follows

$$
\begin{aligned}
K\psi_N^{(m+1)} &= -w_N^{(m)}, \\
\left[I - \delta t\left(Re\left\{\mathscr{F}(\psi^{(m+1)}, \iota)\right\} - K\right)\right] w_N^{(m+1)} &= w_N^{(m)} + \frac{Ha^2}{Re_m}\delta t\left\{\mathscr{F}(A_N^{(m+1)}, J_N^{(m+1)})\right\}, \\
KA_N^{(m+1)} &= -J_N^{(m)}, \\
[I - K\delta t]\, J_N^{(m+1)} &= J_N^{(m)} + Re_m \delta t \mathscr{F}(\psi^{(m+1)}, A_N^{(m+1)}).
\end{aligned}
\tag{3.46}
$$

K is a matrix of order $(N+1)^2 \times (N+1)^2$ defined as $K = I_N \otimes D_N^{(2)} + E_N^{(2)} \otimes I_N$.
I is the identity matrix of size $(N+1)^2$, and ι is the vector whose all entries are 1, and $\mathscr{F}(\phi,\varphi)$ defines the vector constructed by multiplication of the approximations to the first partial derivatives of its argument vectors. $\mathscr{F}(\phi,\varphi)$ is defined as $\mathscr{F}(\phi,\varphi) = \mathrm{D}(E^{(1)}\phi)D^{(1)}\varphi - \mathrm{D}(D^{(1)}\phi)E^{(1)}\varphi$, where D denote the diagonal matrix with the entries of a vector φ on its diagonal.

The final discretized system is iteratively solved. The equation of the stream function is firsly solved by using the initial vorticity values. Thereafter, the velocity components are calculated by the following relation:

$$
u_N^{(m+1)} = \left(E_N^{(1)} \otimes I_N\right) \psi_N^{(m+1)}, \tag{3.47}
$$

$$
v_N^{(m+1)} = -\left(I_N \otimes D_N^{(1)}\right) \psi_N^{(m+1)}. \tag{3.48}
$$

Then, for the vorticity boundary values the following calculation is applied

$$
\left[w_N^{(m+1)}\right]\Big|_s = \left[\left(I_N \otimes D_N^{(1)}\right) v_N^{(m+1)}\right]\Big|_s - \left[\left(E_N^{(1)} \otimes I_N\right) u_N^{(m+1)}\right]\Big|_s, \tag{3.49}
$$

where s denotes the s-th boundary node. Then, the newly obtained stream function values are used in order to obtain the vorticity boundary values. Finally, the updated stream function and vorticity values are used to solve the magnetic stream function and the current density equations. In an analogous way, for the calculation of the current density boundary values the case of vorticity is followed. The magnetic field components are updated first:

$$B_x^{(m+1)} = \left(E_N^{(1)} \otimes I_N\right) A_N^{(m+1)}, \tag{3.50}$$

$$B_y^{(m+1)} = -\left(I_N \otimes D_N^{(1)}\right) A_N^{(m+1)}. \tag{3.51}$$

Then, the current density boundary values are calculated as:

$$\left[J_N^{(m+1)}\right]\Big|_s = \left[\left(I_N \otimes D_N^{(1)}\right) B_y^{(m+1)}\right]\Big|_s - \left[\left(E_N^{(1)} \otimes I_N\right) B_x^{(m+1)}\right]\Big|_s. \tag{3.52}$$

This iterative scheme continues until a convergence tolerance is satisfied within all unknowns between two successive iterations.

3.3. Numerical Results

In this section the numerical solutions to the MHD equations by using CSCM are presented. The solution procedures are implemented by a computer program using MATLAB. First, in Section 3.3.1 the application of CSCM to a one-dimensional flow problem known as MHD Couette flow is considered. Next, in Section 3.3.2 the application of CSCM to the two-dimensional forced MHD flow problem with analytical solution, tests the efficiency of the method and then, provides a comparison with finite difference method (FDM) results obtained by [8]. The application of CSCM to the two-dimensional fluid flow problems, laminar, transient, incompressible MHD flow subjected to an externally applied magnetic field, with attention to the induced magnetic field in a regularized lid-driven cavity is considered in Section 3.3.3. For this case, an artificial time t dependence on the problem is introduced to provide an approximate iterative solution to the governing equations. These equations are given in terms of the stream function ψ, the vorticity w, magnetic stream function A, the current density J, and are solved by an iterative procedure based on CSCM. For the time discretization, an implicit backward finite difference scheme is used. The systems of equations in each iteration, are solved using optimized solver and for all cases the convergence tolerance for this test problem is taken as 10^{-5} for all the unknowns involved in the system, at very points of the problem domain with the use of a time step $\delta t = 0.25$.

3.3.1. One-Dimensional MHD Couette Flow

As first test, a one-dimensional flow problem known as MHD Couette flow is considered and studied to explore the interaction of electric, magnetic, and hydrodynamic forces in the fluid. Here, an electrically conducting fluid is assumed to flow between two parallel plates, one of which is moving its own plane with a constant velocity. The flow is subjected to an external magnetic field applied in the $+y$-direction. Under these considerations, the equation governs the flow is given non-dimensionally as [25]

$$\frac{d^2u}{dy^2} - Ha^2 u = \alpha. \tag{3.53}$$

Here, u is the velocity of the fluid, Ha is the Hartmann number and α is the constant pressure in non-dimensional form. The solution of (3.53) will be approximated by CSCM as follows

$$(\mathfrak{D}^2 - Ha^2 I)u = \alpha \iota, \tag{3.54}$$

where ι is the vector of size $N+1$ whose all components are 1. For this problem, the approximate solution u_N will be compared with the exact solution to (3.53) that is given as [25]

$$u_{\text{exact}} = \frac{\sinh(Hay)}{\sinh(Ha)} + \frac{\alpha}{Ha^2}\left[\frac{2\sinh\left(\frac{Hay}{2}\right)\sinh\left(\frac{Ha(y-1)}{2}\right)}{\cosh\left(\frac{Ha}{2}\right)}\right]. \tag{3.55}$$

The relative error is calculated as follows:

$$E_R = \frac{\|u_{\text{exact}} - u_N\|_\infty}{\|u_{\text{exact}}\|_\infty}, \tag{3.56}$$

where u_N is the approximation to u.

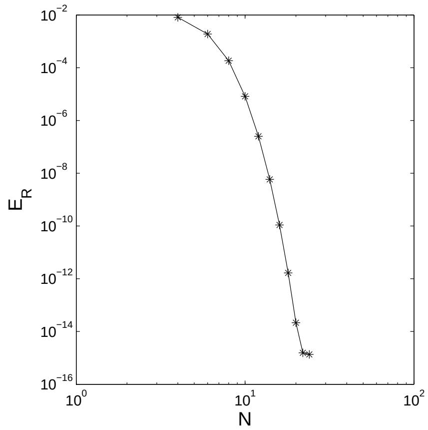

Figure 3.2: Plot of the convergence test for problem 3.3.1.

Figure 3.2 shows the graph of the convergence test in the logarithmic scale for the relative error where $Ha = 10$, $\alpha = 4$, and N varying from 4 to 24 with a step size of 2. From this figure it is evidenced that as N increases the relative error E_R decreases exponentially, which is also termed as spectral convergence. Let us note here that, for the values of N greater than 22, obviously the numerical scheme captures the analytical behaviour of the velocity exactly up to the machine zero.

To explore the effect of the Hartmann number on the flow, we carry out the numerical simulations for $Ha = 1, 2, 5$, and 10, for a fixed value of $\alpha = 1$. The results are depicted in Figure 3.3. This figure puts forward the well known flattening tendency of the magnetic field. As Ha increases, the velocity values decrease on the whole domain. This behaviour is pronounced in the neighborhood of $y = 0.8$.

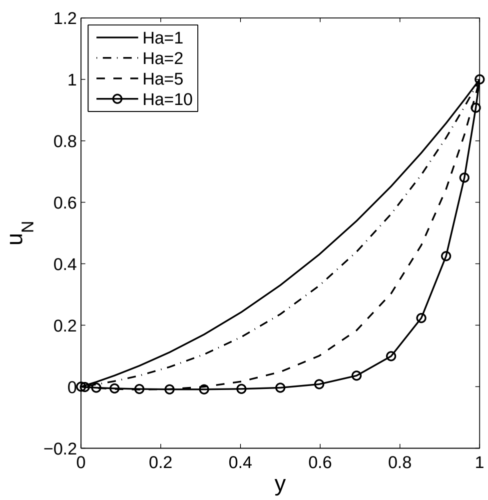

Figure 3.3: The effect of Ha on u_N, where $\alpha = 1$, for problem 3.3.1.

3.3.2. Two-Dimensional Forced MHD Flow Problem With Analytical Solution

As a second numerical test, the application of CSCM to the two-dimensional forced MHD flow problem on the square domain $(0,1)^2$, with analytical solution is presented to test the efficiency of the scheme, and to provide a comparison with the results obtained in the literature.

The problem we consider is defined as follows

$$\begin{aligned} \Delta\psi &= -w, \\ \Delta w &= Re\left(\frac{\partial\psi}{\partial y}\frac{\partial w}{\partial x} - \frac{\partial\psi}{\partial x}\frac{\partial w}{\partial y}\right) - \chi_a, \\ \Delta A &= -J, \end{aligned} \tag{3.57}$$

where χ_a is the additional force term given by $\chi_a = 4Ree^{x+y}$. In this case, the analytical solution is given as [8]

$$\psi = u = -v = e^{x+y}Re,\ A = (x+y)^2,\ B_x = -B_y = 2(x+y). \tag{3.58}$$

The boundary conditions are obtained by the use of this analytical solution. The CSCM formulation can be obtained by using similar steps given in Section 3.2. Here, χ_a is approximated by $(\chi_N)_{ij}$. Therefore, the second equation in (3.57) is approximated by

$$d_{ij}^{(2)}(w_N)_{ij} + e_{ij}^{(2)}(w_N)_{ij} = ReG_{ij} - (\chi_N)_{ij}, \tag{3.59}$$

where G_{ij} is given as (3.40). As the problem is defined on $0 \le x, y \le 1$, the CGL points in x- direction are given as

$$x_i^{CGL} = \frac{1}{2}\cos\left(\frac{i\pi}{N}\right) + \frac{1}{2}, \quad \text{where } i = 0, 1, \ldots, N, \tag{3.60}$$

likewise in y- direction as

$$y_j^{CGL} = \frac{1}{2}\cos\left(\frac{j\pi}{N}\right) + \frac{1}{2}, \quad \text{where } j = 0, 1, \ldots, N. \tag{3.61}$$

For this test, $Re = 1$, $Ha = 5$, and $Re_m = 100$, is considered. Table 3.1 presents the

Table 3.1: $||R - R_{exact}||_2$, where $R = \psi, u, v, A, B_x, B_y, w$, for problem 3.3.2.

	Yu et al. 65×65 (4th order)	CSCM 12×12
ψ	8.139×10^{-11}	1.9223×10^{-11}
u	1.058×10^{-9}	3.6984×10^{-10}
v	1.057×10^{-9}	4.0309×10^{-10}
A	7.933×10^{-11}	2.3979×10^{-11}
B_x	1.997×10^{-10}	1.1023×10^{-9}
B_y	1.997×10^{-10}	2.3128×10^{-9}
w	-	4.5151×10^{-11}

comparison of the numerical results obtained by the present method with the ones obtained in [8] using a method based on FDM. In the case of CSCM, $N = 12$ is used while in the case of FDM, $N = 65$ is used. These results comply with the conventionally known properties of the CSCM. It produces a faster convergence (namely, spectral convergence) compared to local methods (such as FDM) with a fairly reasonable number of collocation points.

3.3.3. Two-Dimensional Full MHD Equations

This section deals with the approximation of full MHD equations given in (3.32). As already noted, the complexity arises mainly because of the nonlinearities in these equations, and the divergence-free constraint for both the velocity and the magnetic fields are to be satisfied. Consequently, it is of great important to design efficient numerical methods and algorithms to solve this problem. Consider CSCM simulation of two-dimensional, steady, laminar, incompressible MHD flow in a following regularized lid-driven cavity. This is a setting widely used in incompressible flow models where the boundary conditions are smoothed in such a way that the velocity and its derivatives vanish at the corners.

The CSCM introduced in Section 3.1 is applied to the two-dimensional MHD equations given in (3.33). The CGL points in x- and y-directions are given as (3.60) and (3.61) respectively.

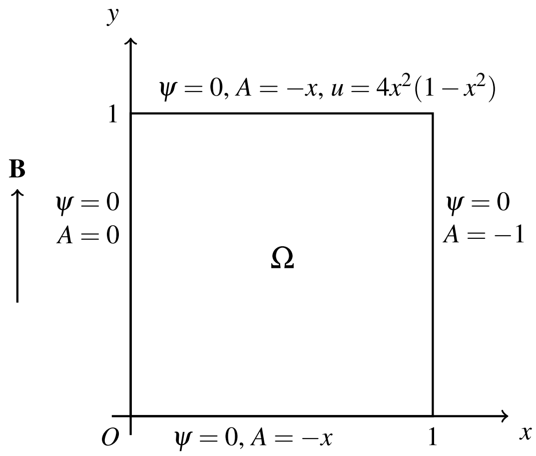

Numerical tests are performed for Hartmann numbers $Ha = 10$, 100, Reynolds numbers $Re = 100$, 1000, and magnetic Reynolds numbers $Re_m = 0.1$, 100.

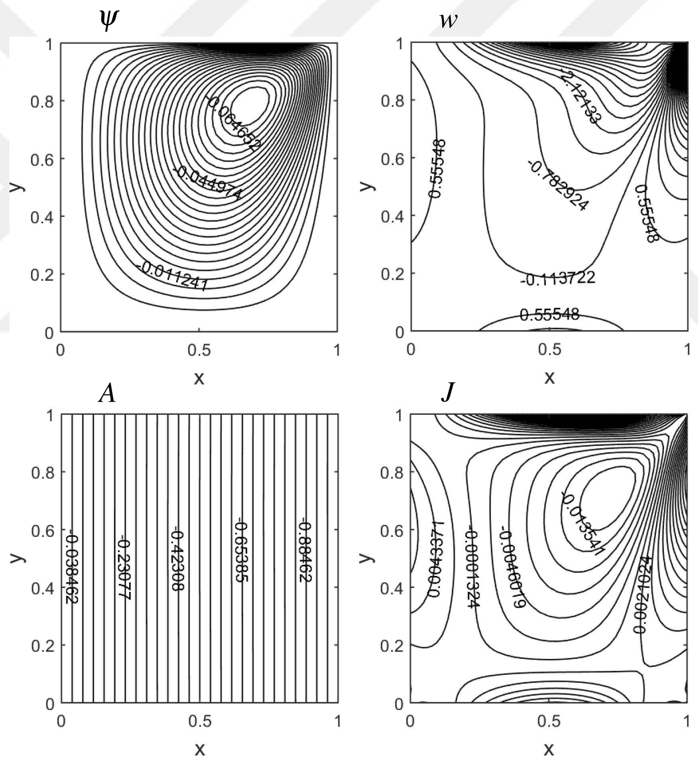

Figure 3.4: CSCM solutions where $Ha = 10$, $Re = 100$, and $Re_m = 0.1$, for problem 3.3.3.

For the first numerical test, the divergence-free conditions are given as $\|\nabla.\mathbf{B}\|_2 = 8.1034 \times 10^{-10}$ and $\|\nabla.\mathbf{u}\|_2 = 1.0585 \times 10^{-7}$. It is seen that the divergence-free conditions are satisfied in regards to the given tolerance. Figure 3.4 presents the numerical results in terms of the contours of the unknowns for $Ha = 10$, $Re = 100$, and $Re_m = 0.1$. It is observed that both stream function and vorticity contours start to get condensed close to the upper right as the upper lid moving. At low values of magnetic Reynolds number $Re_m = 0.1$, the induced magnetic field lines are straight in the $+y$-direction. The induced magnetic field is dominated by the applied magnetic field.

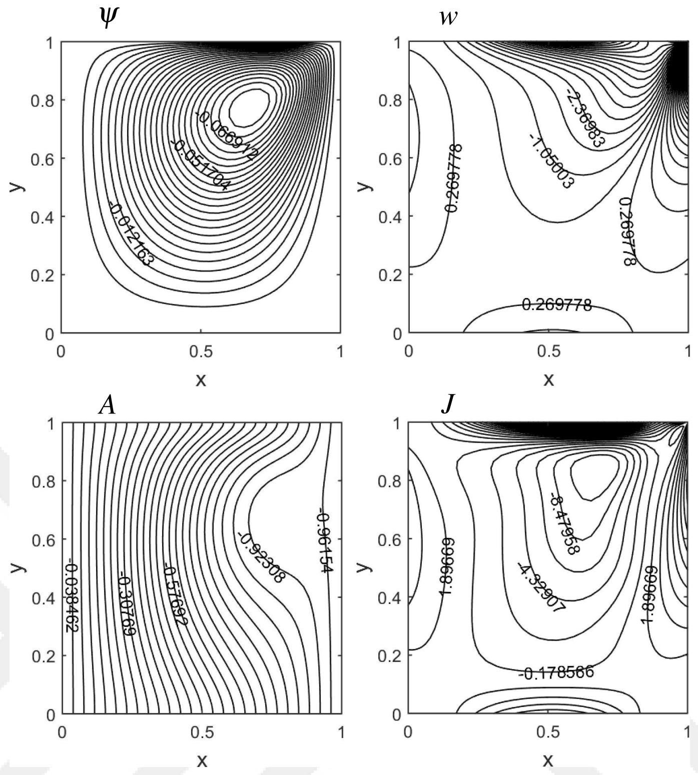

Figure 3.5: The effect of magnetic Reynolds number $Re_m = 100$, when $Ha = 10$, and $Re = 100$, for problem 3.3.3.

For the second numerical test, the divergence-free conditions are given as $\|\nabla.\mathbf{B}\|_2 = 5.4798 \times 10^{-10}$ and $\|\nabla.\mathbf{u}\|_2 = 9.556 \times 10^{-8}$. It is observed that the divergence-free conditions are satisfied. Figure 3.5 shows the behaviour of stream function, vorticity, magnetic stream function and current density for $Ha = 10$, $Re = 100$, and $Re_m = 100$. It is seen that stream function and vorticity are not altered much with the increase in Re_m because the corresponding equations do not have a direct dependence on Re_m. Moreover, it can be observed that current density forms circulations when Re_m increases because of the strong Lorentz force effect. Furthermore, the magnetic induction lines start to circulate inside the channel due to the increasing values of $Re_m = 100$.

For the third numerical test, the divergence-free conditions are given as $\|\nabla.\mathbf{B}\|_2 = 5.358 \times 10^{-10}$ and $\|\nabla.\mathbf{u}\|_2 = 8.1733 \times 10^{-8}$. It is seen that the divergence-free conditions are satisfied. Figure 3.6 presents the numerical results in terms of the contours of the unknowns for $Ha = 100$, $Re = 1000$, and $Re_m = 100$. From this figure it can be

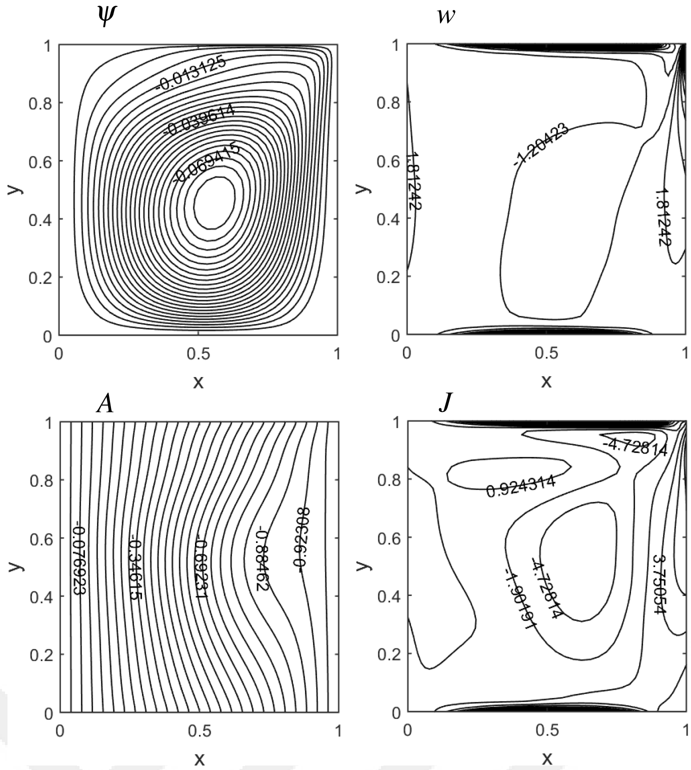

Figure 3.6: The effect of Hartmann number $Ha = 100$ and Reynolds number $Re = 1000$, when $Re_m = 100$, for problem 3.3.3.

seen that formation of boundary layers near the walls of the cavity for both the vorticity and the current density because of the applied magnetic field intensity. The vortex in the flow formed along the center due to the increasing values of Hartman number $Ha = 100$ and Reynolds number $Re = 1000$. It is also observed that the induced magnetic field lines start up smoothly due to the high value of Hartmann number. All these results agree reasonably well with the previous published results (e.g. [1]-[9]).

As a conclusion, in this chapter, some conceptual discussions relating to the main themes of the work which are CSCM and MHD flow equations are presented. Further, the applications of these concepts are also presented in this chapter. It is realized that, the results obtained from the use of the CSCM are more accurate and simpler to compute than those obtained by local methods in Section 3.3.2. The efficiency and simplicity associated with the CSCM in the computations aided in solving the full MHD equations. It is shown that the flow behaviour in the cavity as well as the contour magnitudes of all the unknowns are in good agreement with the literature results. Moreover, it is seen that the vortex of the fluid moves through the center as Ha and Re increase. Besides, the effects of the Re_m on the magnetic field and current density are reduced. The magnetic field distribution in the cavity is not affected much by increasing the Re_m

to moderate values. However, for large Re_m, a strong circulation takes place near the upper right region of the cavity. The numerical results obtained, reveal the fact that the numerical procedure based on CSCM approximates the full MHD equations effectively. Moreover, the divergence-free nature of the magnetic field is shown to be preserved on the computational domain.

4. CONCLUSION

This study aims at numerical solutions for solving the MHD flow problems. A CSCM is presented for approximating the full MHD equations. The CSCM is a collocation method which depends on polynomial interpolation and the differentiation of this polynomial. The CSCM is based on the fact that interpolating polynomials are defined on a set of clustered CGL points (collocation points) to approximate the unknown functions, in which the differential equations are discretized. The polynomials are analytically differentiated and for derivative approximation a differentiation matrix is constructed. The approximations to the higher order derivatives are obtained by multiplying the lower order differentiation matrices.

Chapter two focuses on polynomial interpolation and the significance of the choice of interpolation points for enhancement of accuracy. The Lagrange polynomial interpolation with equispaced points is presented. Subsequently, the Runge phenomenon is observed and the solution to the problem arising from this phenomenon is discussed by choosing special points. Moreover, Chebyshev polynomials as well as the points to be used in the interpolation are also presented. Polynomial approximation in the infinity norm is used to determine differences in the function and its interpolating polynomial. Consequently, the best approximation of degree N is stated with examples. Thereafter, the Lebesgue function which is the summation of the absolute value of Lagrange basis functions is evaluated. The Lebesgue constant, defined as the maximum of Lebesgue function depends on the interpolation points and gives an idea on the closeness of Lagrange interpolation polynomial to the best approximation polynomial is also evaluated. For this purpose, three sets of points are used, namely, the equispaced points, the CG points, and the CGL points. Notably, computation of Lebesgue constant indicated that the CGL points are the most accurate among the mentioned three sets of points. Differentiation of the interpolation polynomial is presented and illustrated by examples.

In the third chapter, numerical solutions of MHD flow equations using CSCM are presented. In this part one-and two-dimensional laminar flows of viscous and incompressible fluids are considered. The one-dimensional MHD flow known as Couette flow that explores the interaction of electric, magnetic, and hydrodynamic forces in the fluid, is considered firstly. Then, the CSCM solutions to the problems of steady, two-dimensional MHD flow in a regularized lid-driven cavity are presented. The MHD flow is subjected to an externally applied magnetic field, where the induced magnetic field is also considered. The governing equations are coupled, nonlinear system of PDEs and are given in non-dimensional form in terms of the stream function ψ, the vorticity w, the magnetic stream function A, and the current density J. An iterative procedure is designed for the purpose of estimating the physically unavailable vorticity and current density boundary conditions. Wherein, the divergence-free condition for the magnetic field is satisfied automatically on the whole problem domain. In order to provide an approximate solution to these equations by an iterative scheme, an artificial time t dependence on the problem is introduced. Then, an implicit backward finite difference scheme is used for time discretization. It is noteworthy that the results obtained by two-dimensional test using CSCM in the present study, are more accurate and simpler to compute than those previously reported by [8] using FDM. The simplicity and efficiency associated with the CSCM in the computations aided in solving the full MHD equations. It is shown that the flow behaviour in the cavity as well as the contour magnitudes of all the unknowns are in good agreement with the literature results. The divergence-free nature of the magnetic field is shown to be preserved on the whole computational domain. The numerical results obtained from one and two-dimensional MHD flow problems indicate that the designed procedure based on CSCM, approximates the full MHD equations efficiently.

REFERENCES

[1] Bozkaya N., Tezer-Sezgin M., (2011), “The DRBEM solution of incompressible MHD flow equations”, International Journal for Numerical Methods in Fluids, 67(10), 1264-1282.

[2] Shercliff J.A., (1953), “Steady motion of conducting fluids in pipes under transverse magnetic fields”, Mathematical Proceedings of the Cambridge Philosophical Society, 49(1), 136-144.

[3] Armero F., Simo J.C., (1996), “Long-term dissipativity of time-stepping algorithms for an abstract evolution equation with applications to the incompressible MHD and Navier-Stokes equations”, Computer Methods in Applied Mechanics and Engineering, 131(1-2), 41-90.

[4] Liu J.G., Wang W.C., (2001), “An energy-preserving MAC-Yee scheme for the incompressible MHD equation”, Journal of Computational Physics, 174(1), 12-37.

[5] Codina R., Hernandez N., (2011), “Approximation of the thermally coupled MHD problem using a stabilized finite element method”, Journal of Computational Physics, 230(4), 1281-1303.

[6] Türk Ö., Tezer-Sezgin M., (2013), “FEM solution of natural convection flow in square enclosures under magnetic field”, International Journal of Numerical Methods for Heat & Fluid Flow, 23(5), 844-866.

[7] Pekmen B., Tezer-Sezgin M., (2015), “DRBEM solution of MHD flow with magnetic induction and heat transfer”, CMES-Computer Modeling in Engineering & Science, 105(3), 183-207.

[8] Yu P.X., Tian Z.F., Ying A.Y., Abdou M.A., (2017), “Stream function-velocity-magnetic induction compact difference method for the 2D steady incompressible full magnetohydrodynamic equations”, Computer Physics Communications, 219, 45-69.

[9] Türk Ö., (2018), “Chebyshev spectral collocation method approximation to thermally coupled MHD equations”, Süleyman Demirel Üniversitesi Fen Bilimleri Enstitüsü Dergisi, 22, 355-366.

[10] Suli E., Mayers D.F., (2003), “An Introduction to Numerical Analysis”, Cambridge University Press.

[11] Weierstrass K., (1885), "Über die analytische darstellbarkeit sogenannter willkürlicher functionen einer reellen veränderlichen", Sitzungsberichte der Königlich Preußischen Akademie der Wissenschaften zu Berlin, 2, 633-639.

[12] Bernšteın S., (1912), "Démonstration du théorème de Weierstrass fondée sur le calcul des probabilités", Comm. Soc. Math. Kharkov, 13, 1-2.

[13] Runge C., (1901), "Über empirische funktionen und die interpolation zwischen äquidistanten ordinaten", Zeitschrift für Mathematik und Physik, 46(224-243), 20.

[14] Brown J.W., Churchill R.V., (2009), "Complex Variables and Applications", 8th Edition, McGraw-Hill.

[15] Trefethen L.N., (2000), "Spectral Methods in MATLAB", SIAM.

[16] Gheorghiu C.I., (2007), "Spectral Methods for Differential Problems", Casa Cartii de Ştiinta.

[17] Burden R.L., Faires J.D., (2010), "Numerical Analysis", 9th Edition, Brooks Cole, Boston, MA.

[18] Gautschi W., (2011), "Numerical Analysis", 2nd Edition, Birkhäuser Basel.

[19] Erdös P., (1961), "Problems and results on the theory of interpolation II", Acta Mathematica Hungarica, 12, 235-244.

[20] Trefethen L.N., Weideman J.A.C., (1991), "Two results on polynomial interpolation in equally spaced points", Journal of Approximation Theory, 65(3), 247-260.

[21] Günttner R., (1980), "Evaluation of Lebesgue constants", SIAM Journal on Numerical Analysis, 17(4), 512-520.

[22] Hoang N., (2016), "On node distributions for interpolation and spectral methods", Mathematics of Computation, 85(298), 667-692.

[23] Boyd J.P., (2000), "Chebyshev and Fourier Spectral Methods", 2nd Edition, Dover Publications Inc. New York.

[24] Canuto C., Hussaini M.Y., Quarteroni A., Zang T.A., (1988), "Spectral Method in Fluid Dynamics", Springer-Verlag.

[25] Na T.Y., (1980), "Computational Methods in Engineering Boundary Value Problems", Academic Press.

BIOGRAPHY

Ali Ridwanou SERAJOU was born on 9^{th} of January in Brazzaville, Congo. He completed primary and secondary education in Bangui, Central Africa Republic (CAR).

In 2011, he successfully completed the Bachelor of Science Degree in Mathematics, Bangui University, Central Africa Republic. After graduation, he worked as interpreter and Assistant accounting in Libya embassy, CAR.

In 2015, he moved to Turkey to purpose his M.Sc. in Mathematics. In 2016, he obtained a diploma in Turkish language from Kocaeli University, Turkey. In 2017, he started his M.Sc. in Mathematics (Numerical Analysis) at the Graduate School of Natural and Applied Science in Gebze Technical University, Turkey.